Regioselective Oxidation and Metalation of *meso*-Unsubstituted Azuliporphyrins

Venkata A. K. Adiraju, Gregory M. Ferrence and Timothy D. Lash

Department of Chemistry, Illinois State University, Normal, Illinois 61790-4160

E-mail: tdlash@ilstu.edu

Table of Contents

Page

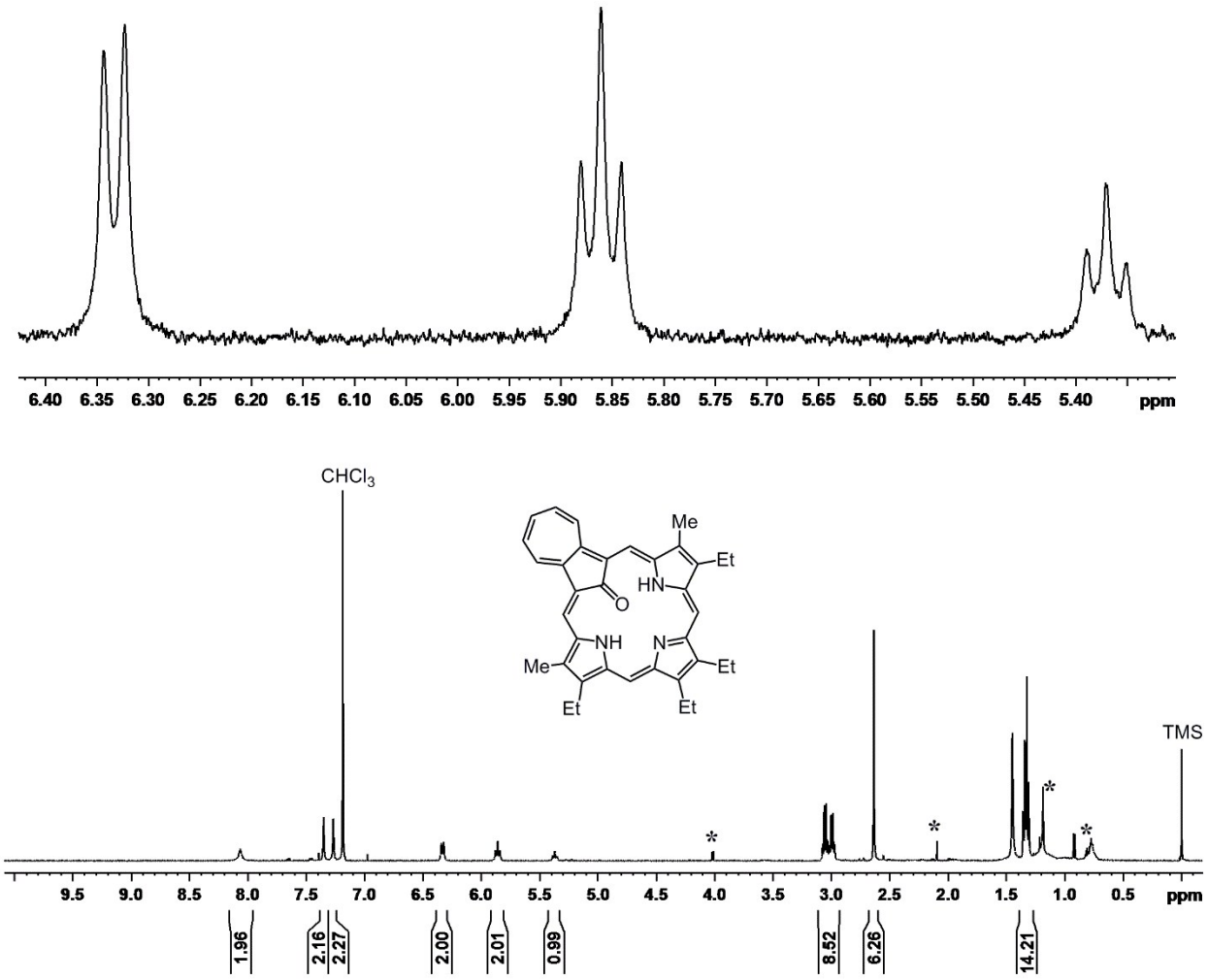

Figure S53. 500 MHz proton NMR spectrum of oxyazuliporphyrin **18b** in $CDCl_3$.
* solvent impurities

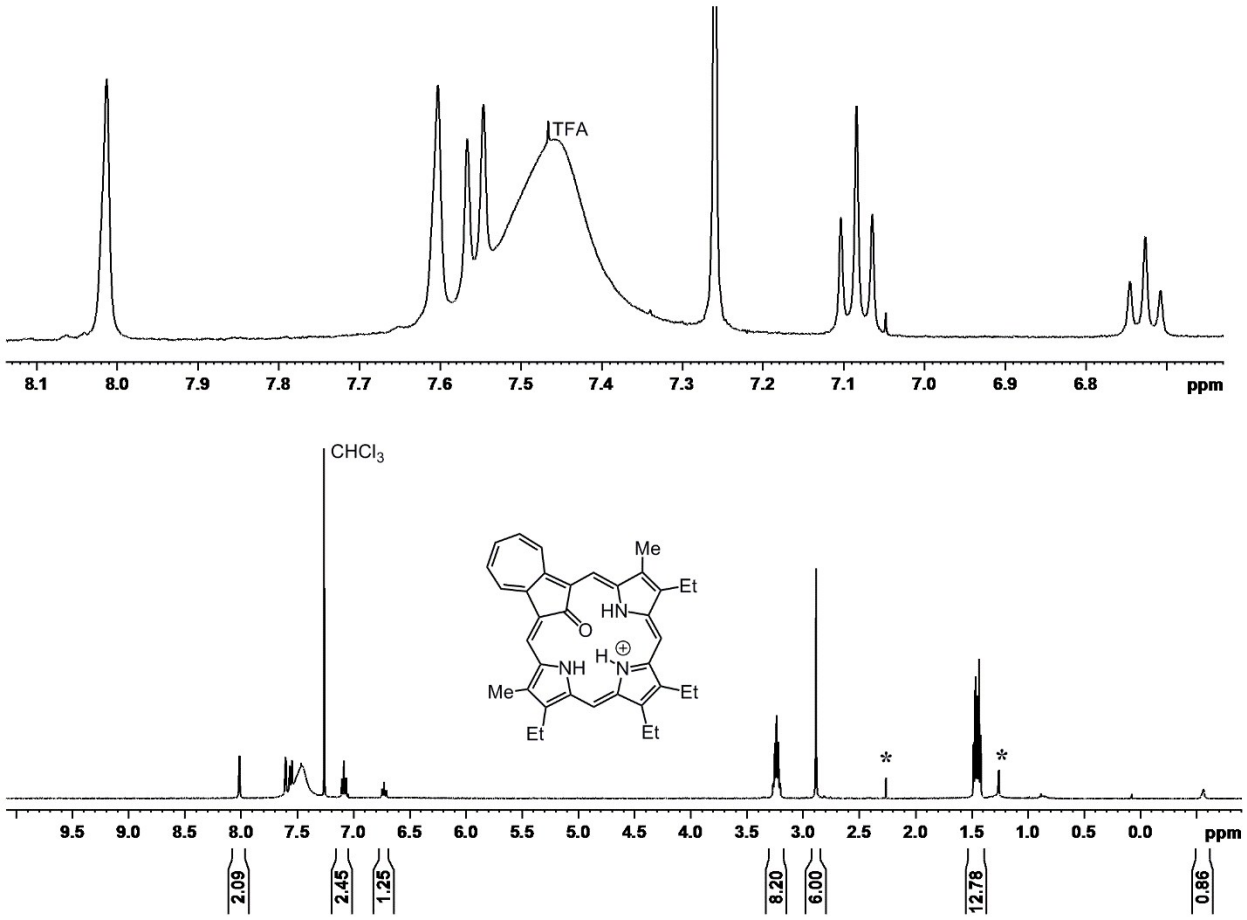

Figure S54. 500 MHz proton NMR spectrum of monoprotonated oxyazuliporphyrin **16b**H^+ in TFA-$CDCl_3$.
* solvent impurities

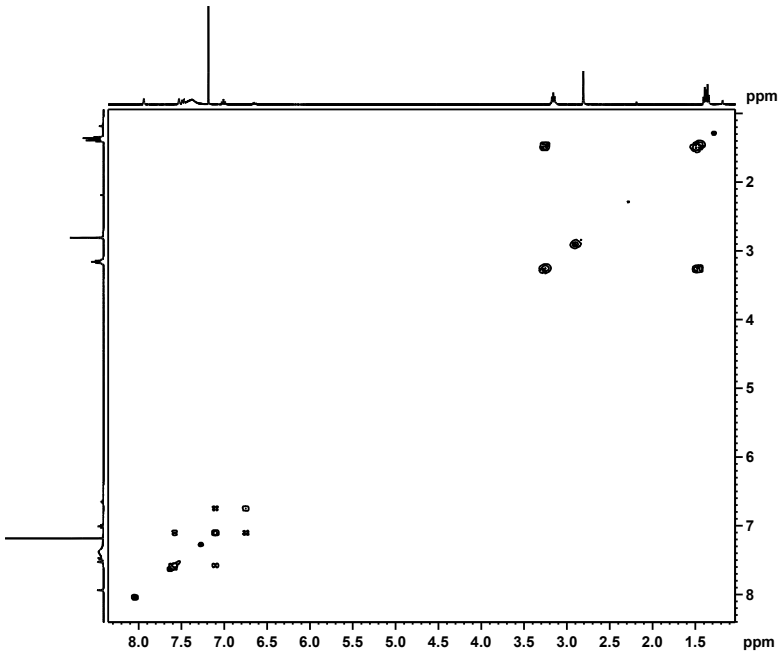

Figure S55. ^{1}H-^{1}H COSY NMR spectrum of **16b**H^{+} in TFA-$CDCl_3$.

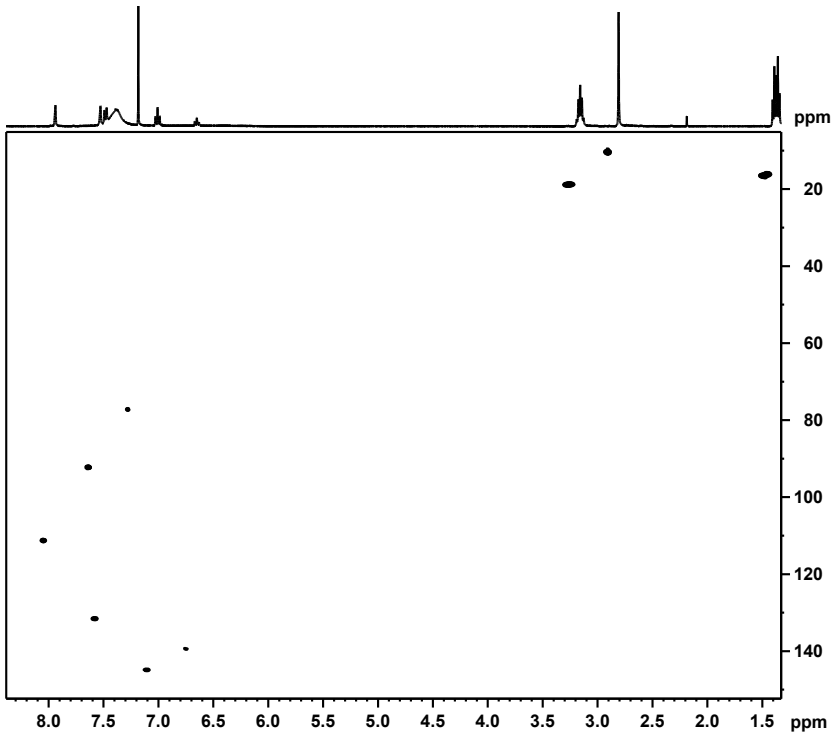

Figure S56. HSQC NMR spectrum of **16b**H^{+} in TFA-$CDCl_3$.

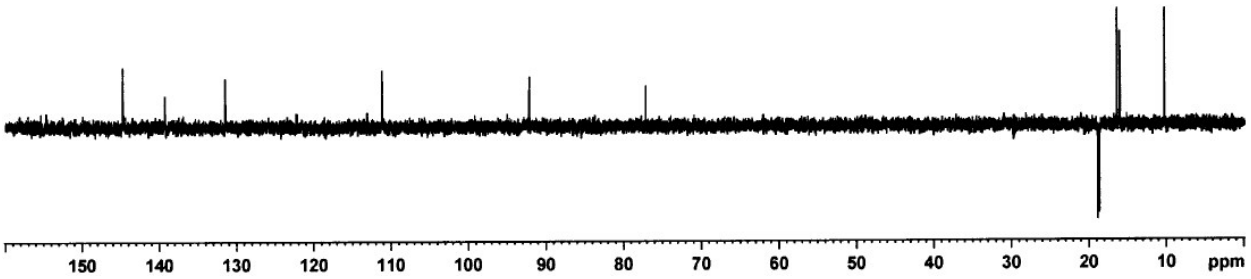

Figure S57. DEPT-135 NMR spectrum of **16b**H^+ in TFA-$CDCl_3$.

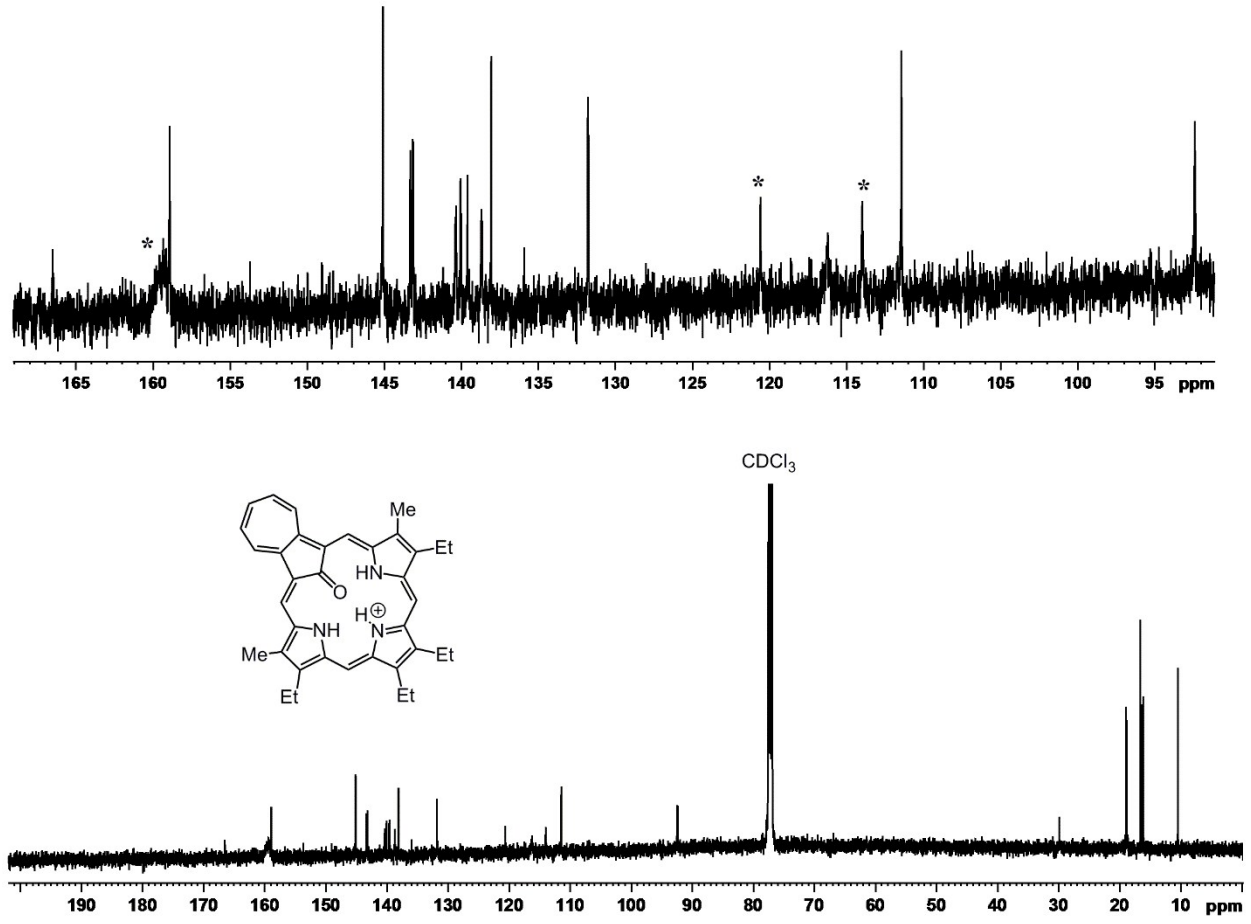

Figure S58. 125 MHz carbon-13 NMR spectrum of **16b**H^+ in trace TFA-$CDCl_3$.
* TFA

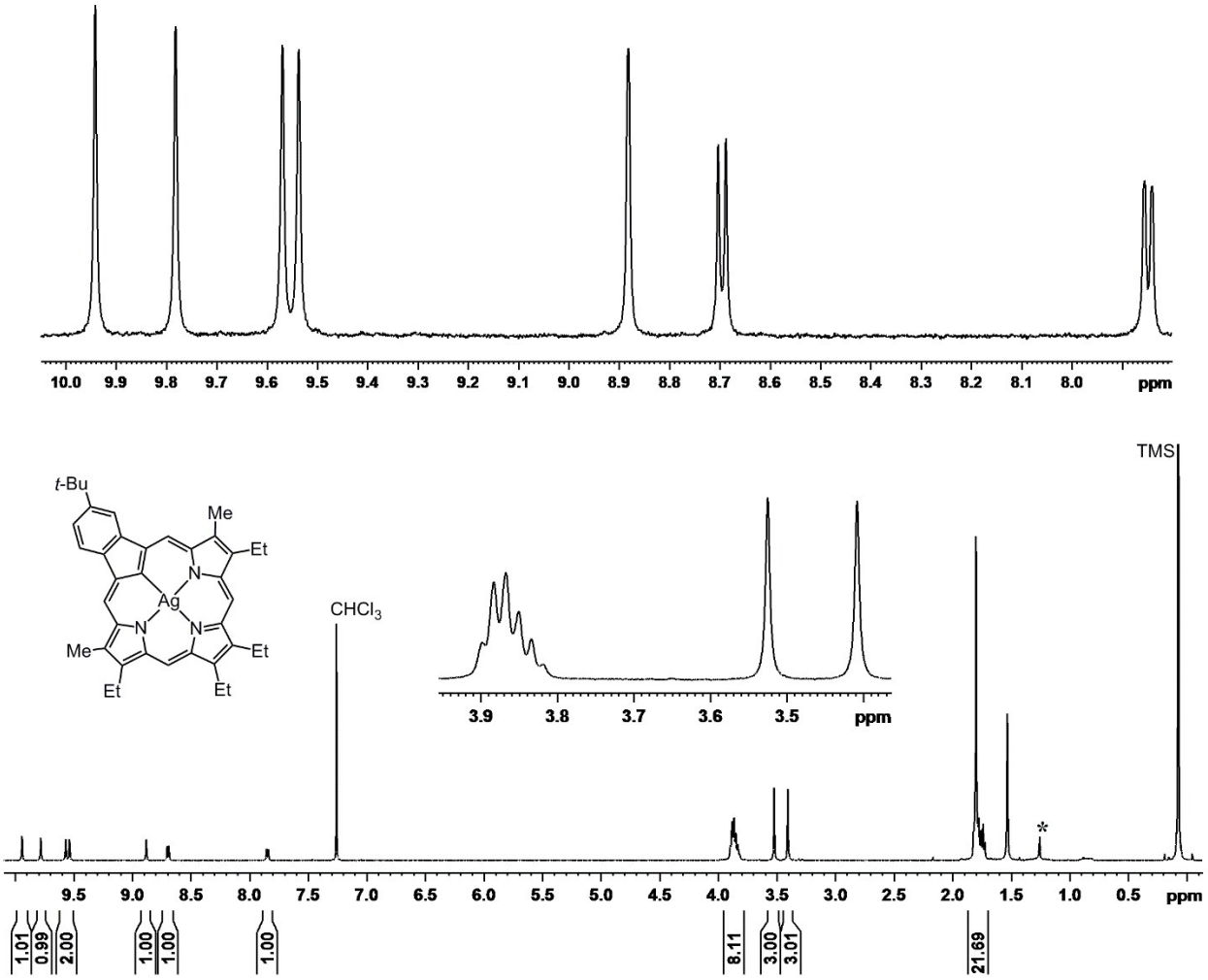

Figure S59. 500 MHz proton NMR spectrum of silver(III) *tert*-butylbenzocarbaporphyrin **21a** in $CDCl_3$.

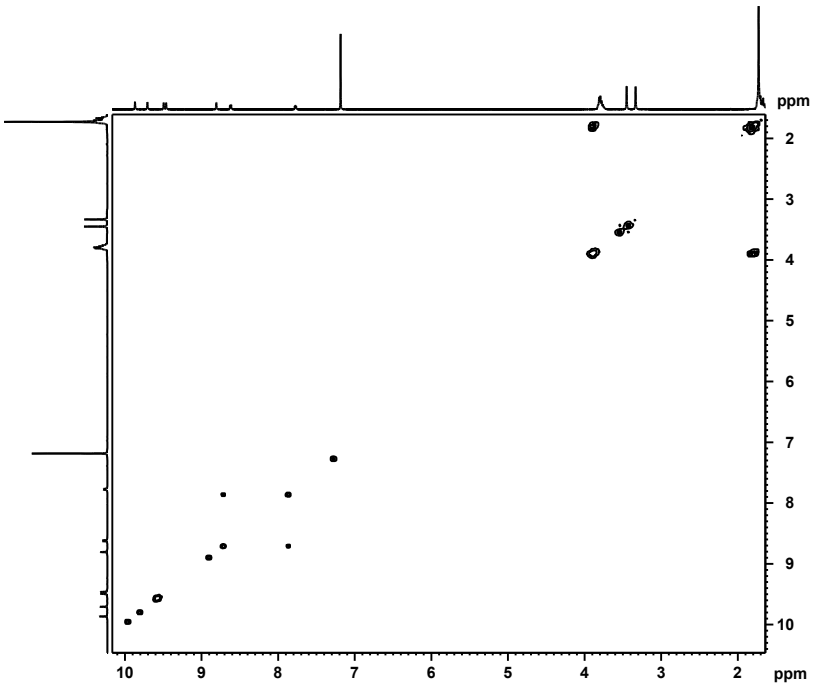

Figure S60. ^{1}H-^{1}H COSY NMR spectrum of silver(III) *tert*-butylbenzocarbaporphyrin **21a** in $CDCl_3$.

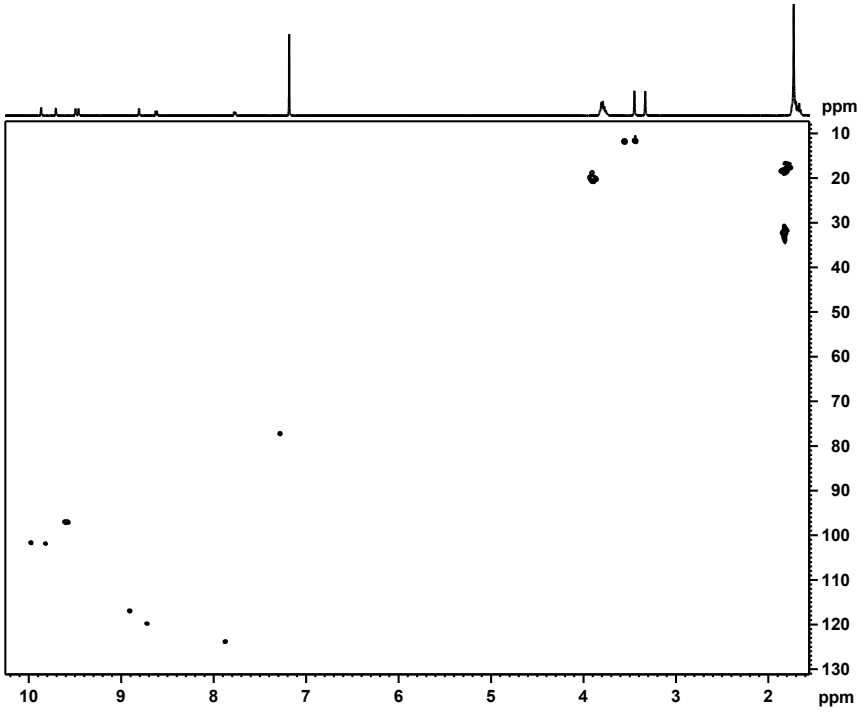

Figure S61. HSQC NMR spectrum of silver(III) *tert*-butylbenzocarbaporphyrin **21a** in $CDCl_3$.

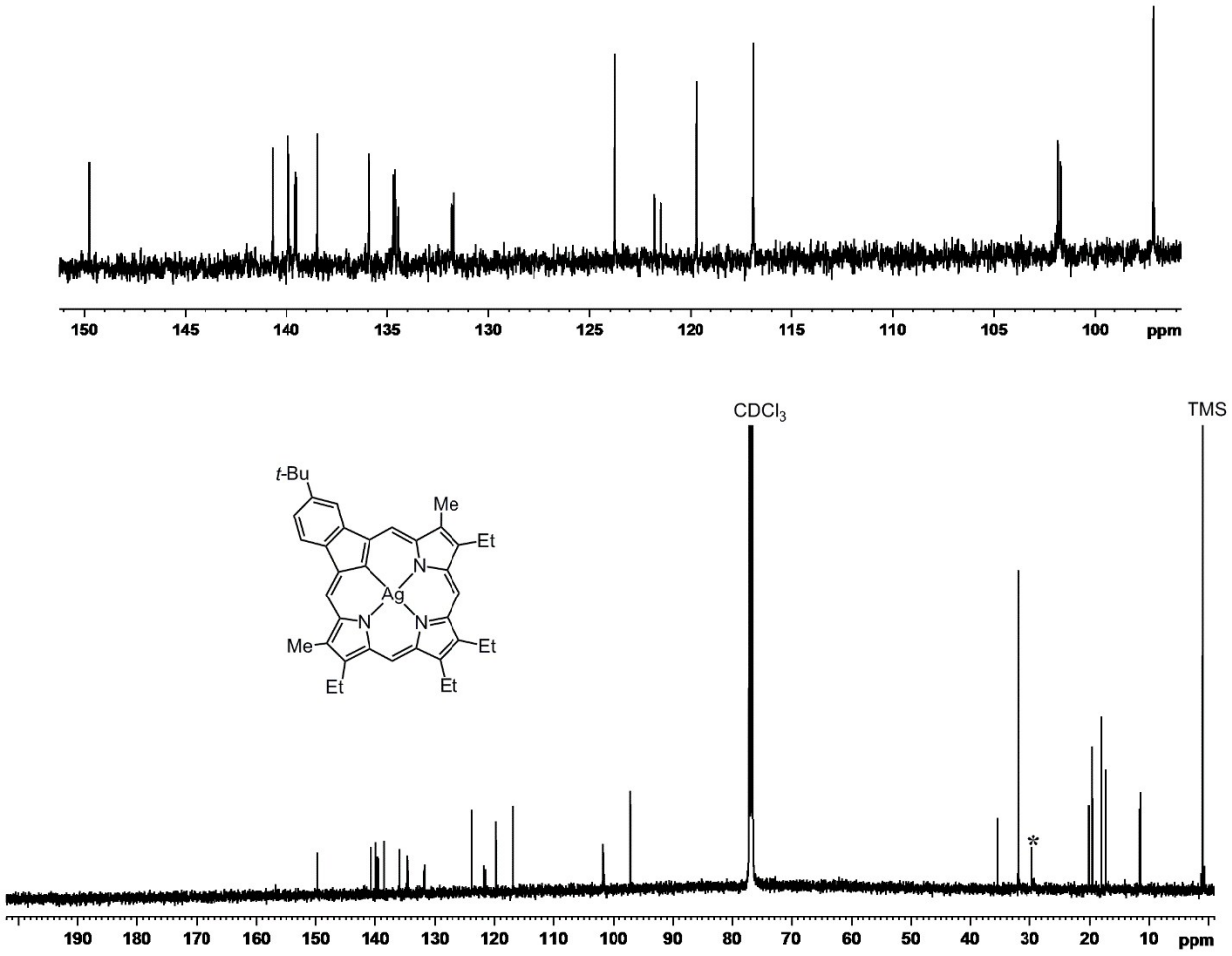

Figure S62. 125 MHz carbon-13 NMR spectrum of silver(III) *tert*-butylbenzocarbaporphyrin **21a** in $CDCl_3$.

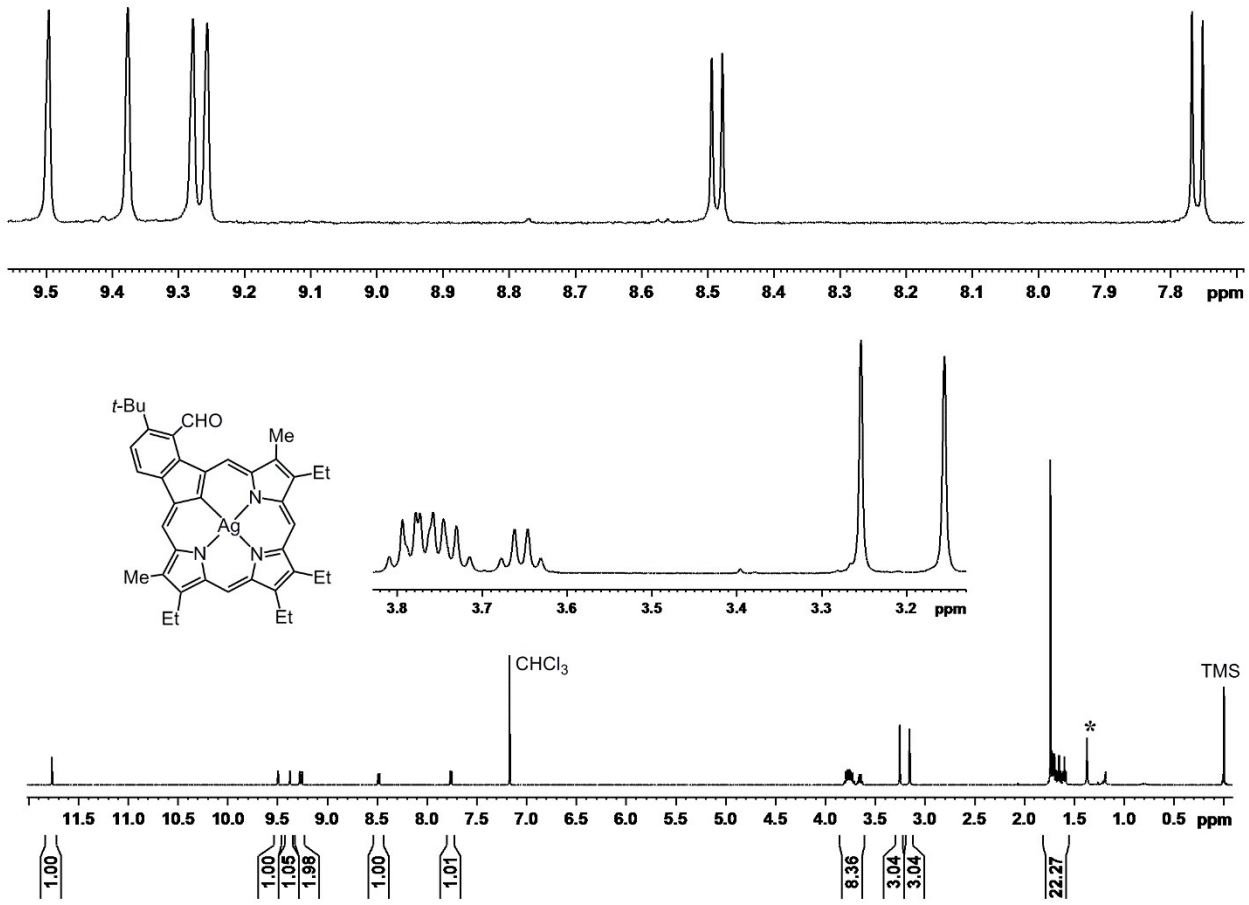

Figure S63. 500 MHz proton NMR spectrum of silver(III) *tert*-butylbenzocarbaporphyrin carbaldehyde **21b** in $CDCl_3$.
* solvent impurity

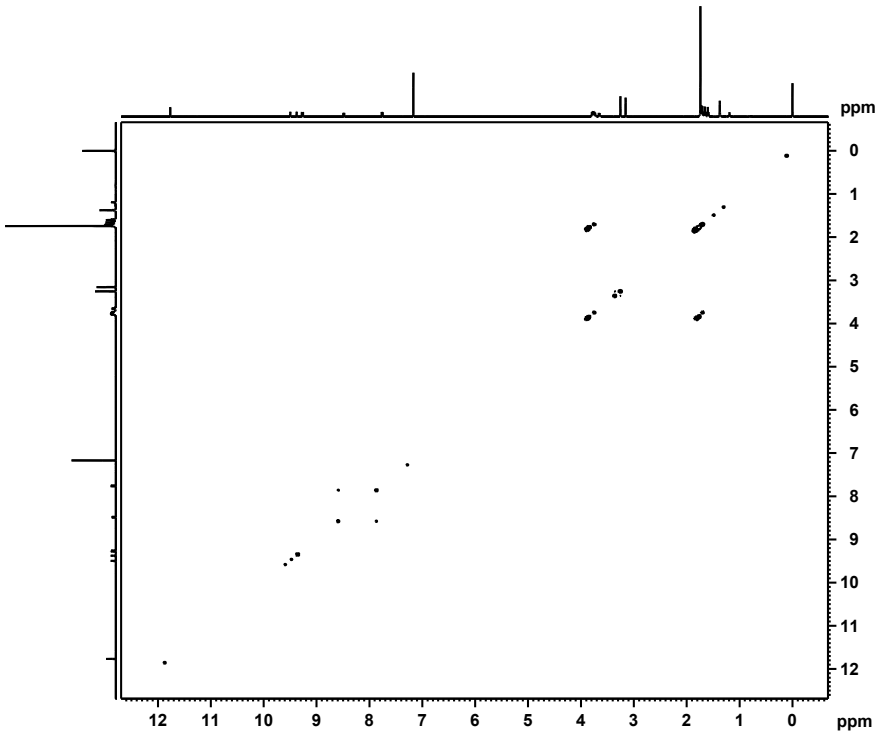

Figure S64. ^{1}H-^{1}H COSY NMR spectrum of **21b** in $CDCl_3$.

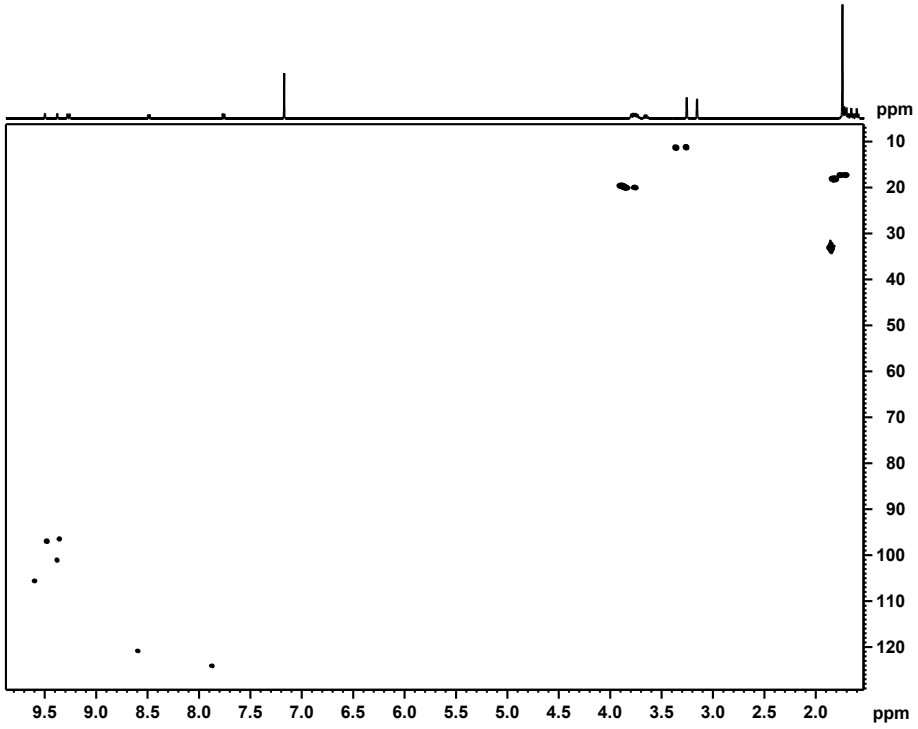

Figure S65. HSQC NMR spectrum of **21b** in $CDCl_3$.

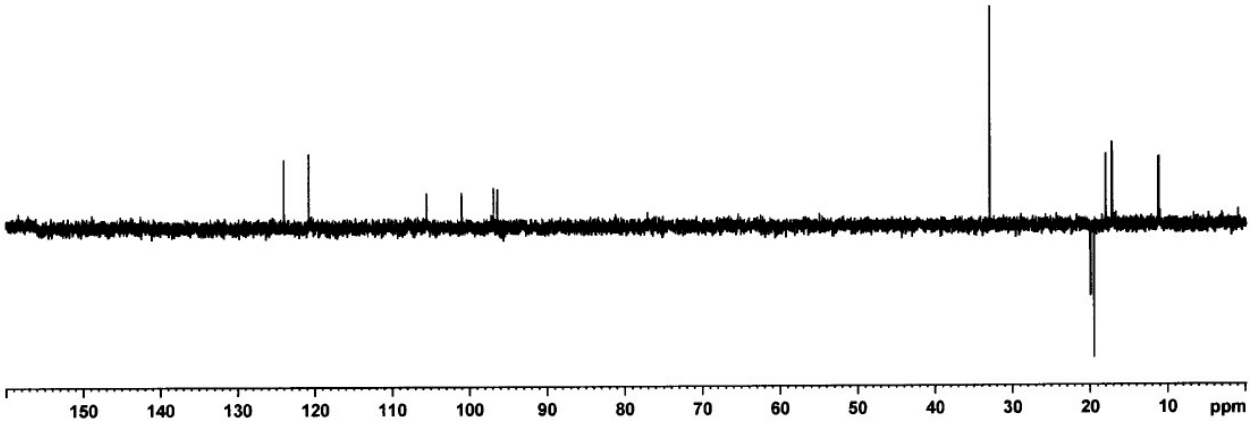

Figure S66. DEPT-135 NMR spectrum of **21b** in $CDCl_3$.

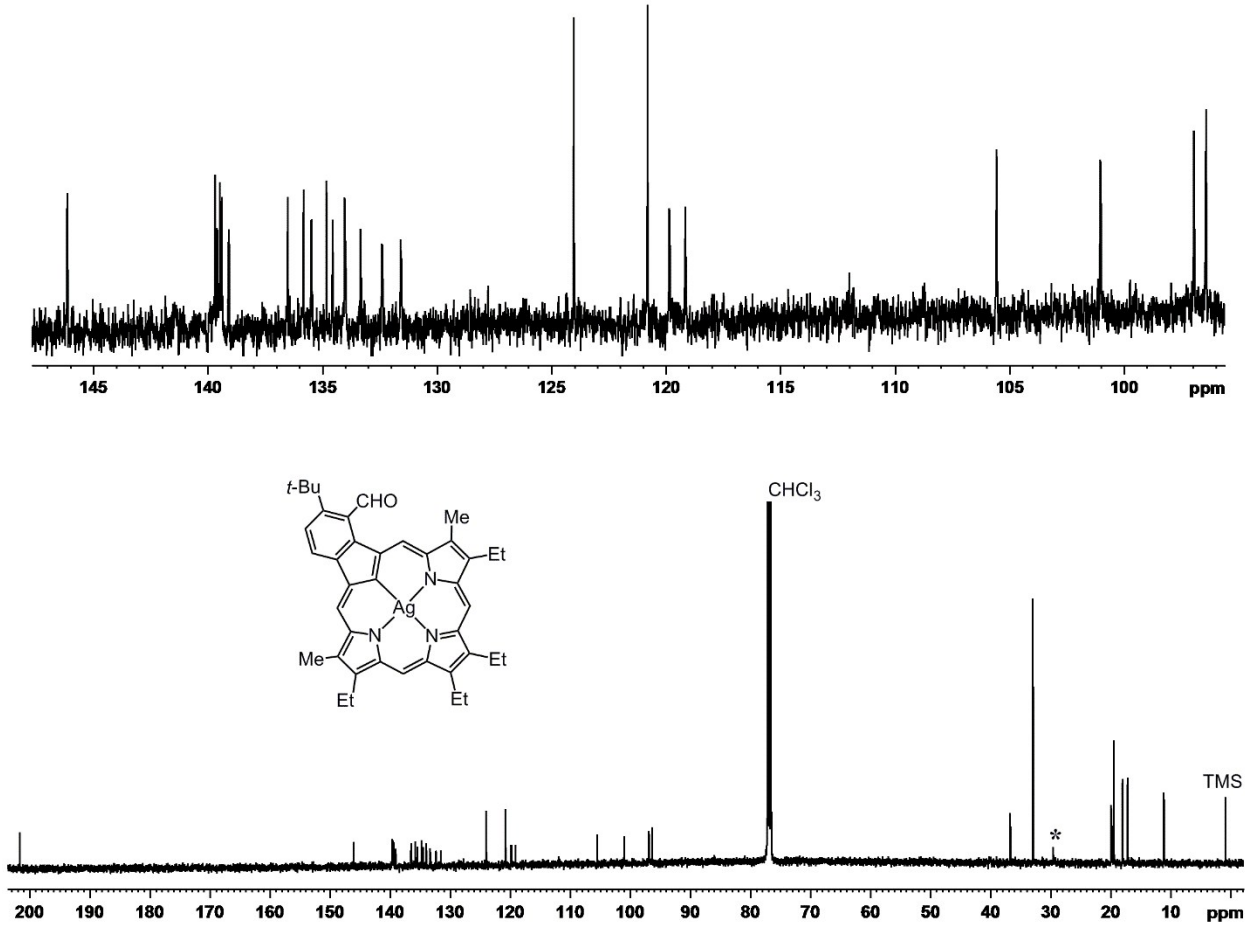

Figure S67. 125 MHz carbon-13 NMR spectrum of silver(III) *tert*-butylbenzocarbaporphyrin carbaldehyde **21b** in $CDCl_3$.

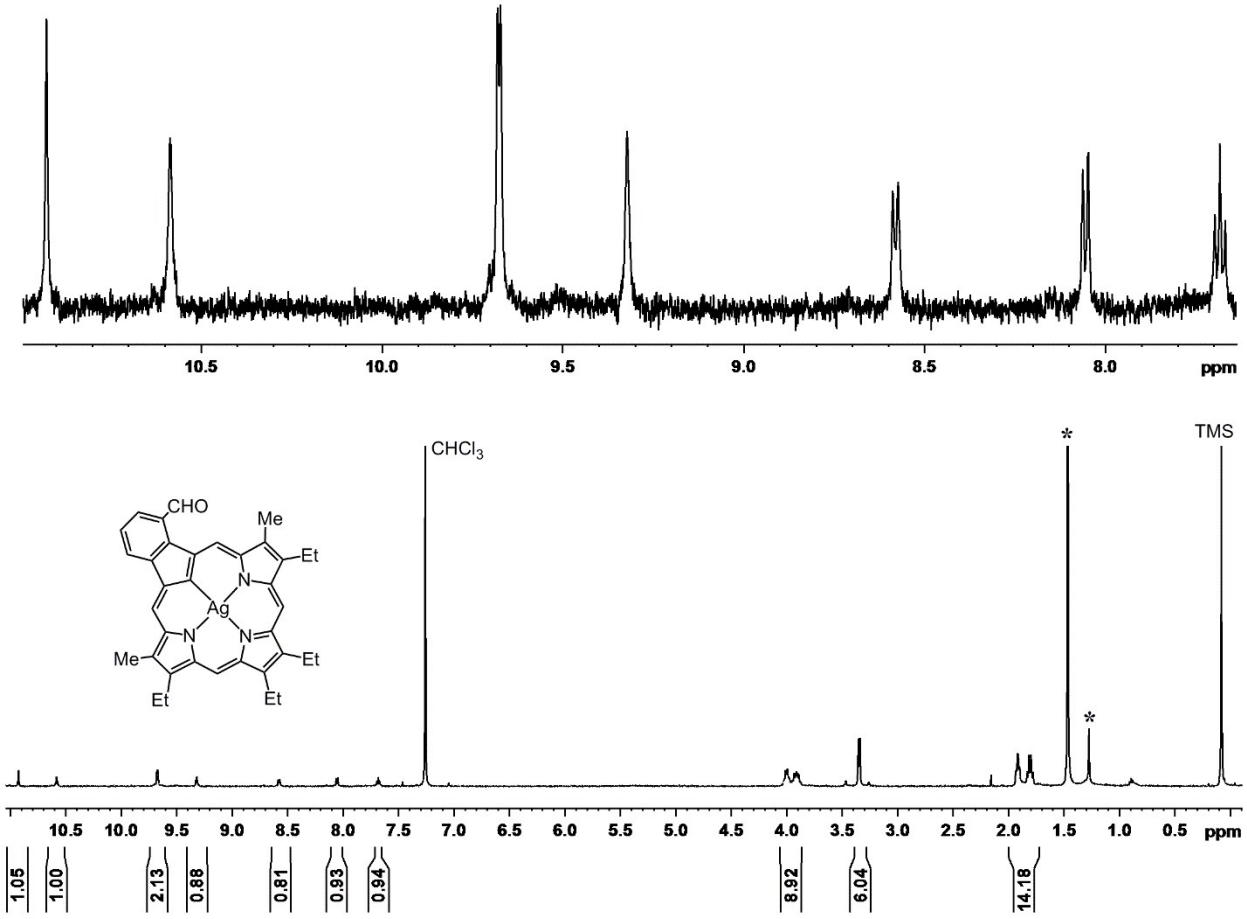

Figure S68. 500 MHz proton NMR spectrum of silver(III) benzocarbaporphyrin carbaldehyde **22c** in $CDCl_3$ at 50 °C. This sample was highly insoluble in organic solvents.
* solvent impurities

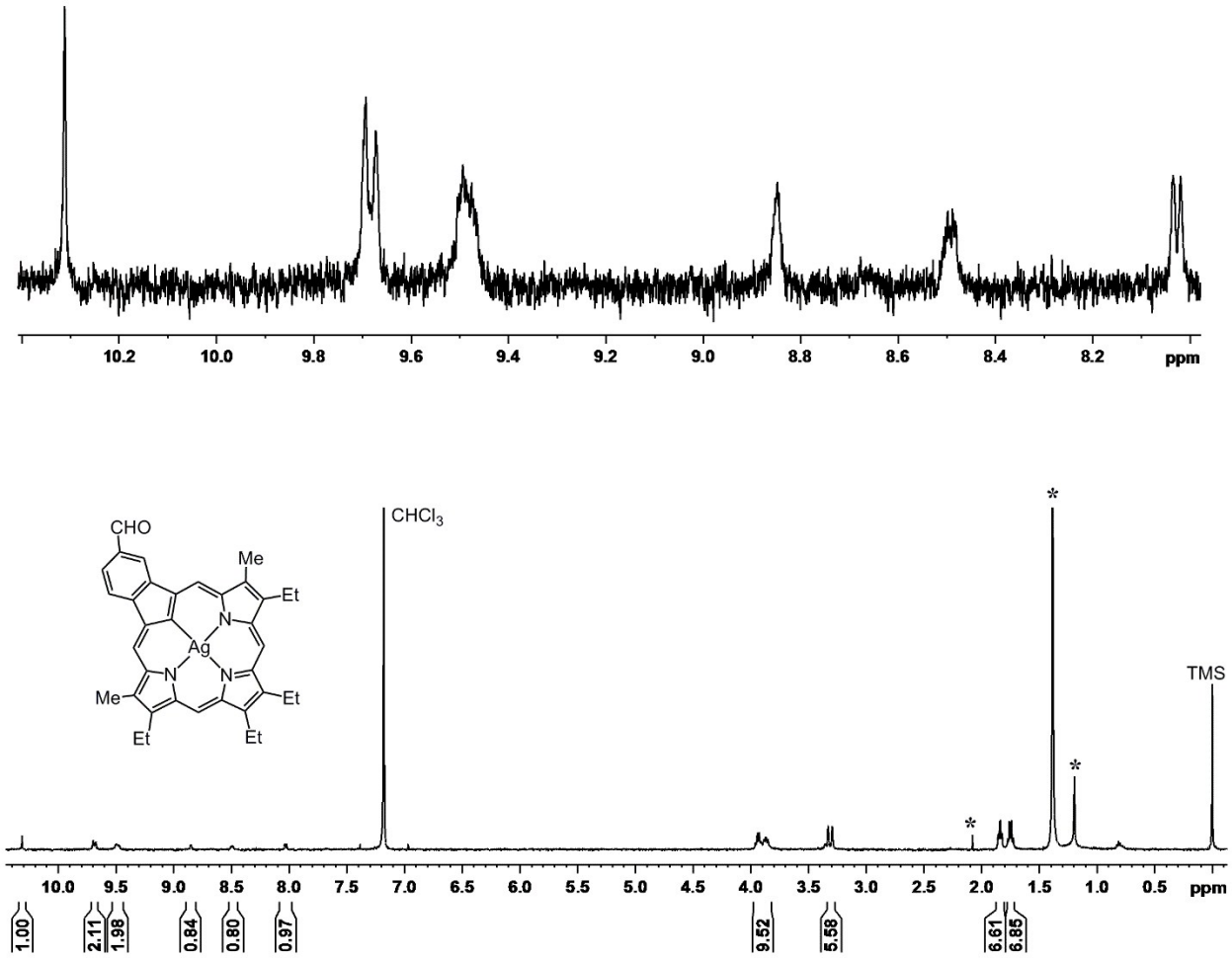

Figure S69. 500 MHz proton NMR spectrum of silver(III) benzocarbaporphyrin carbaldehyde **22b** in $CDCl_3$ at 50 °C. This sample was highly insoluble in organic solvents.
* solvent impurities

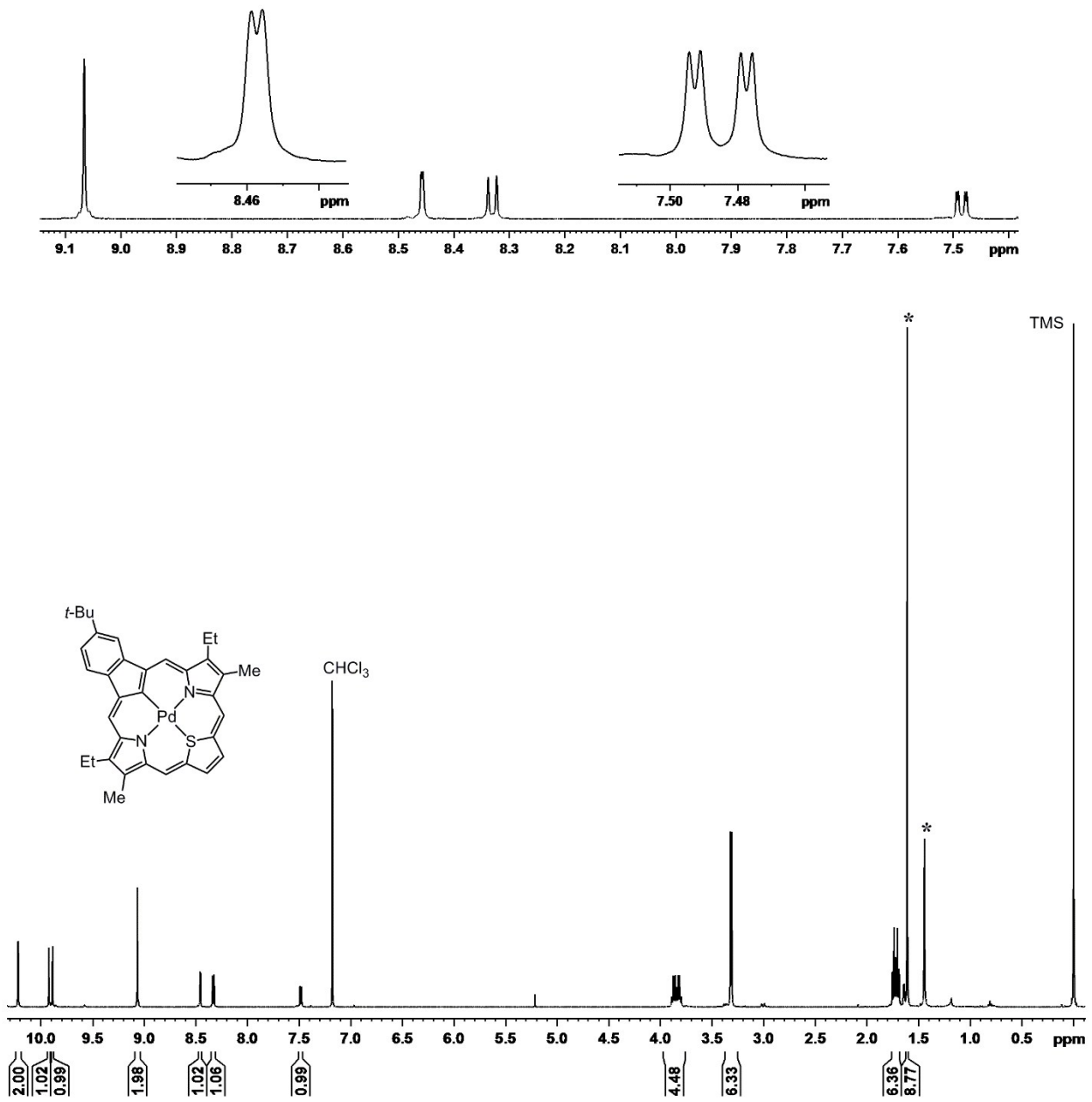

Figure S70. 500 MHz proton NMR spectrum of palladium(II) *tert*-butylbenzocarbaporphyrin **29a** in $CDCl_3$.

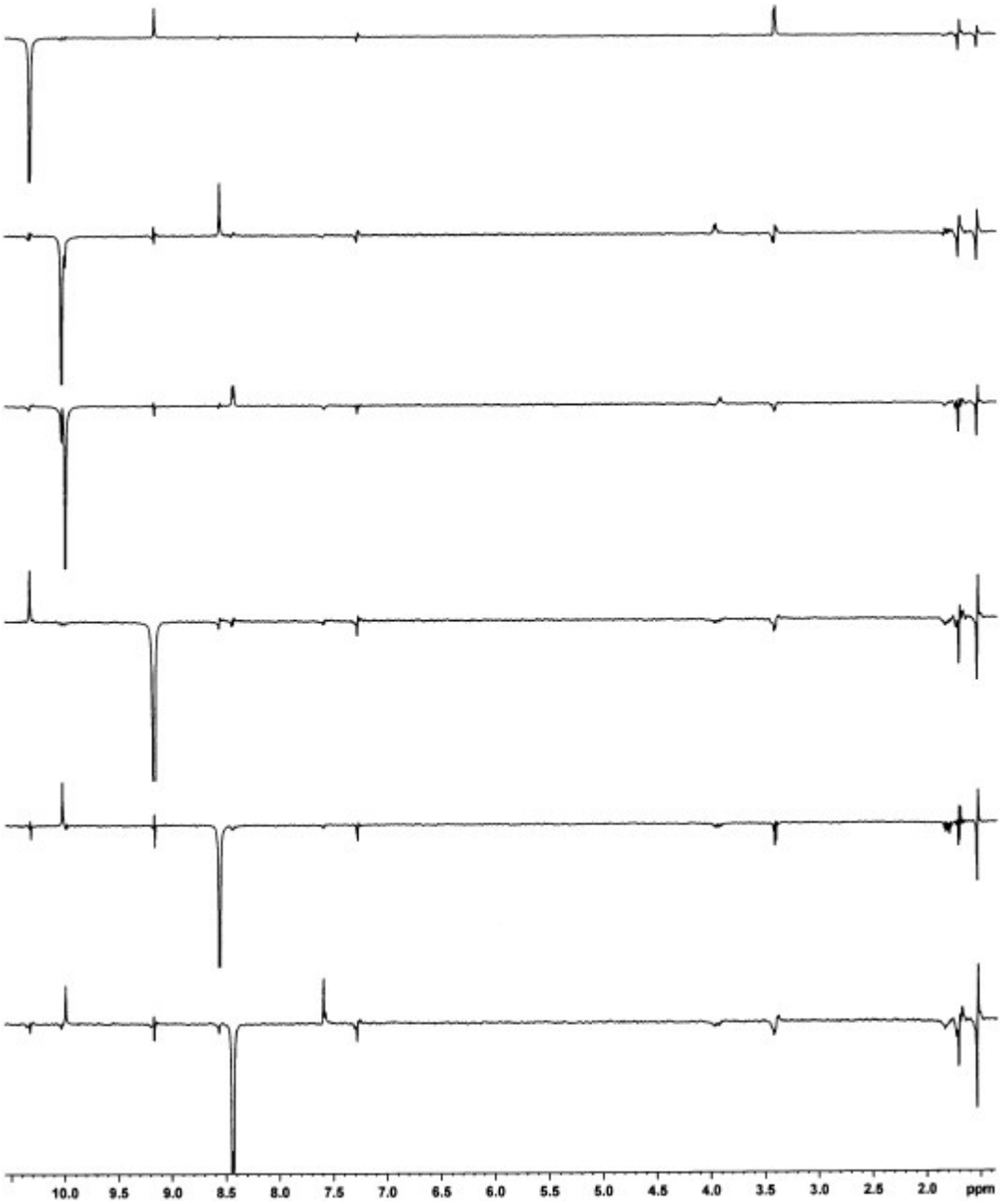

Figure S71. Selected nOe difference proton NMR spectra of palladium(II) *tert*-butyl-benzocarbaporphyrin **29a** in $CDCl_3$.

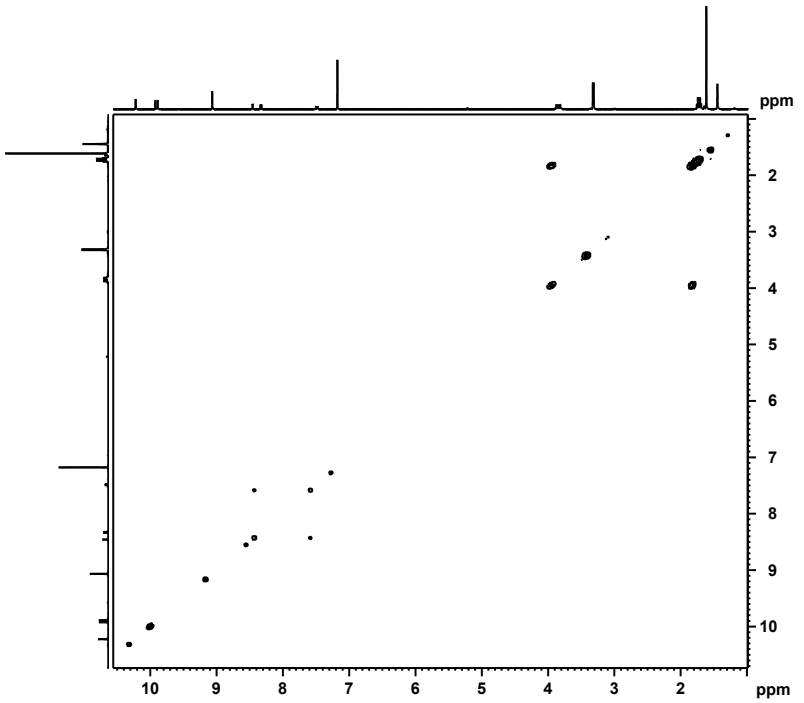

Figure S72. ^{1}H-^{1}H COSY NMR spectrum of palladium(II) complex **29a** in $CDCl_3$.

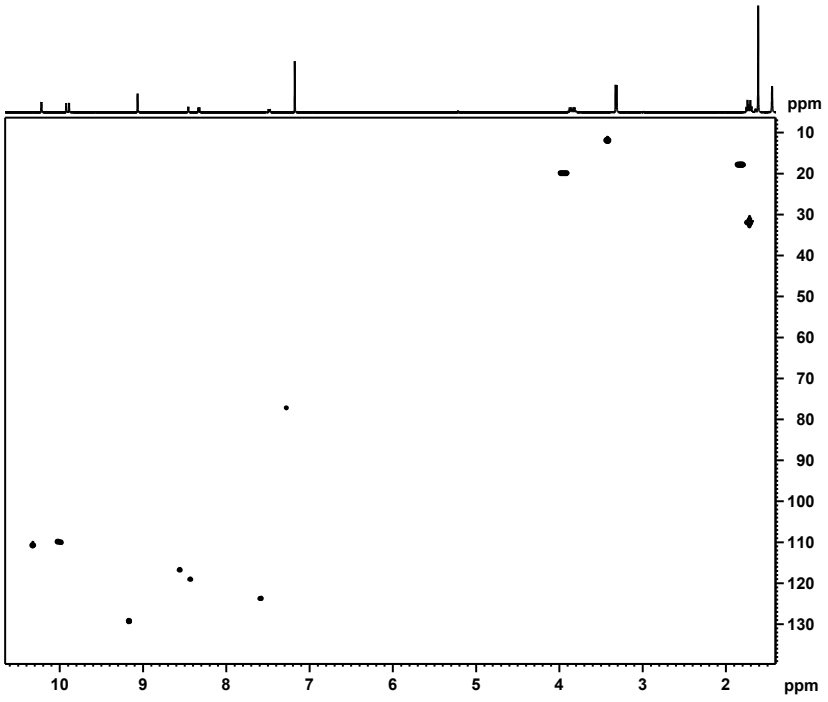

Figure S73. HSQC NMR spectrum of palladium(II) *tert*-butylbenzocarbaporphyrin **29a** in $CDCl_3$.

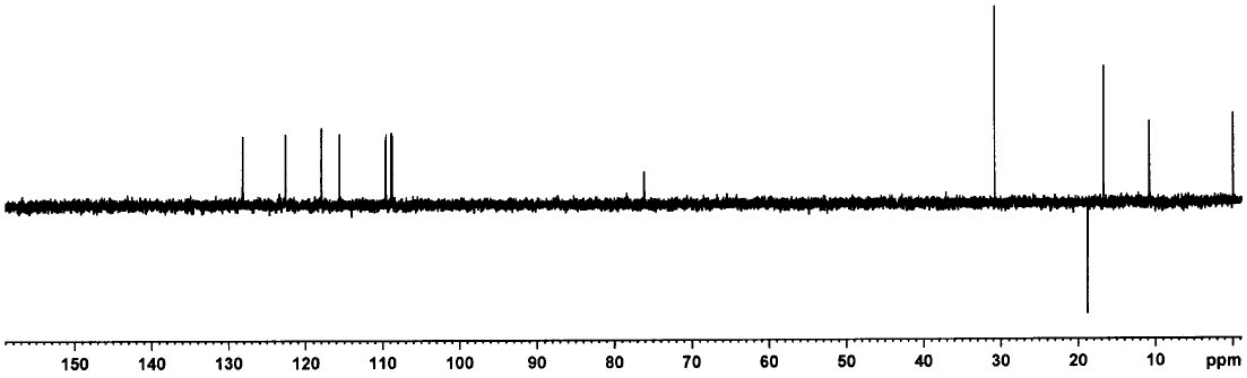

Figure S74. DEPT-135 NMR spectrum of **29a** in $CDCl_3$.

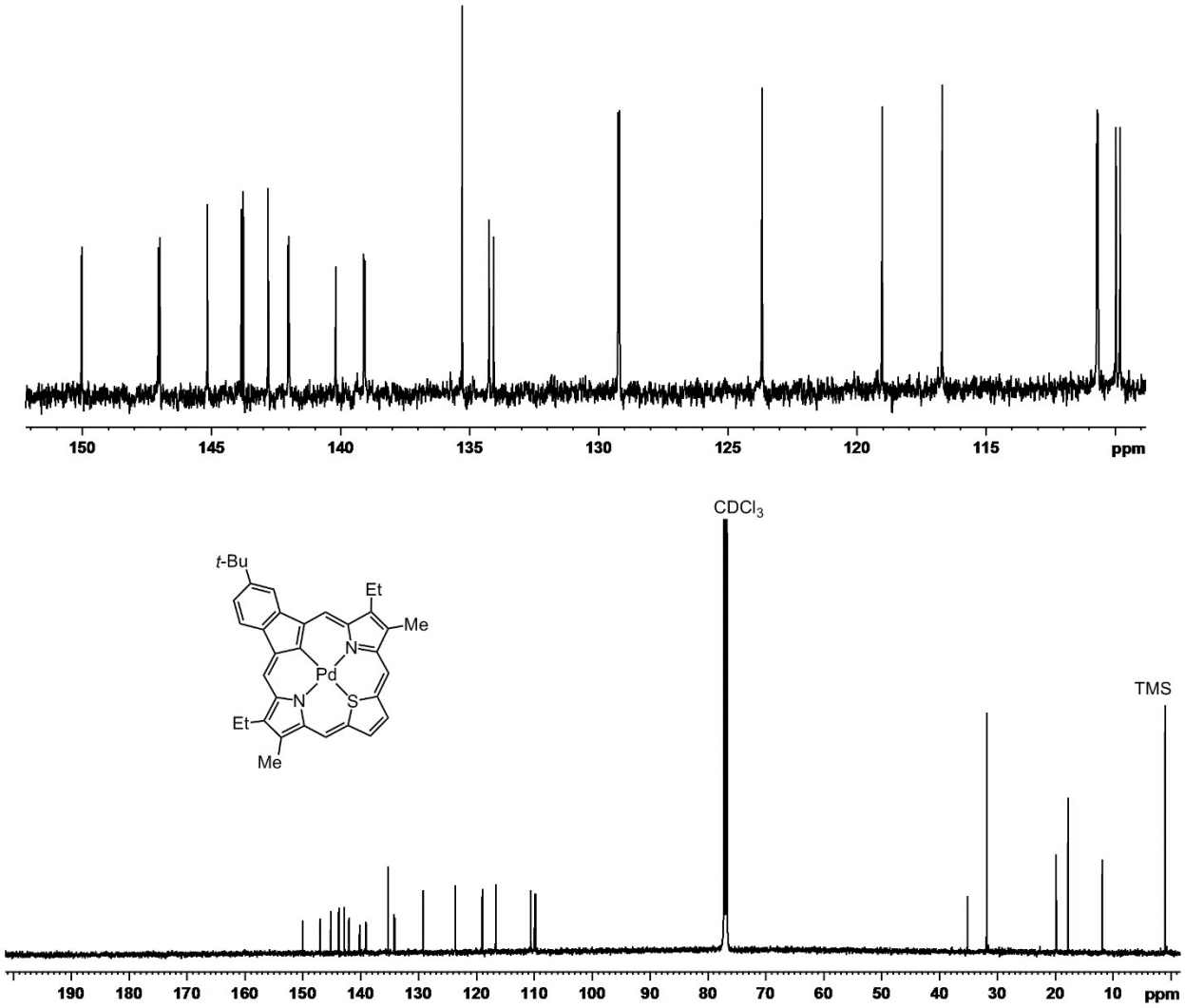

Figure S75. 125 MHz carbon-13 NMR spectrum of palladium(II) *tert*-butylbenzocarbaporphyrin **29a** in $CDCl_3$.

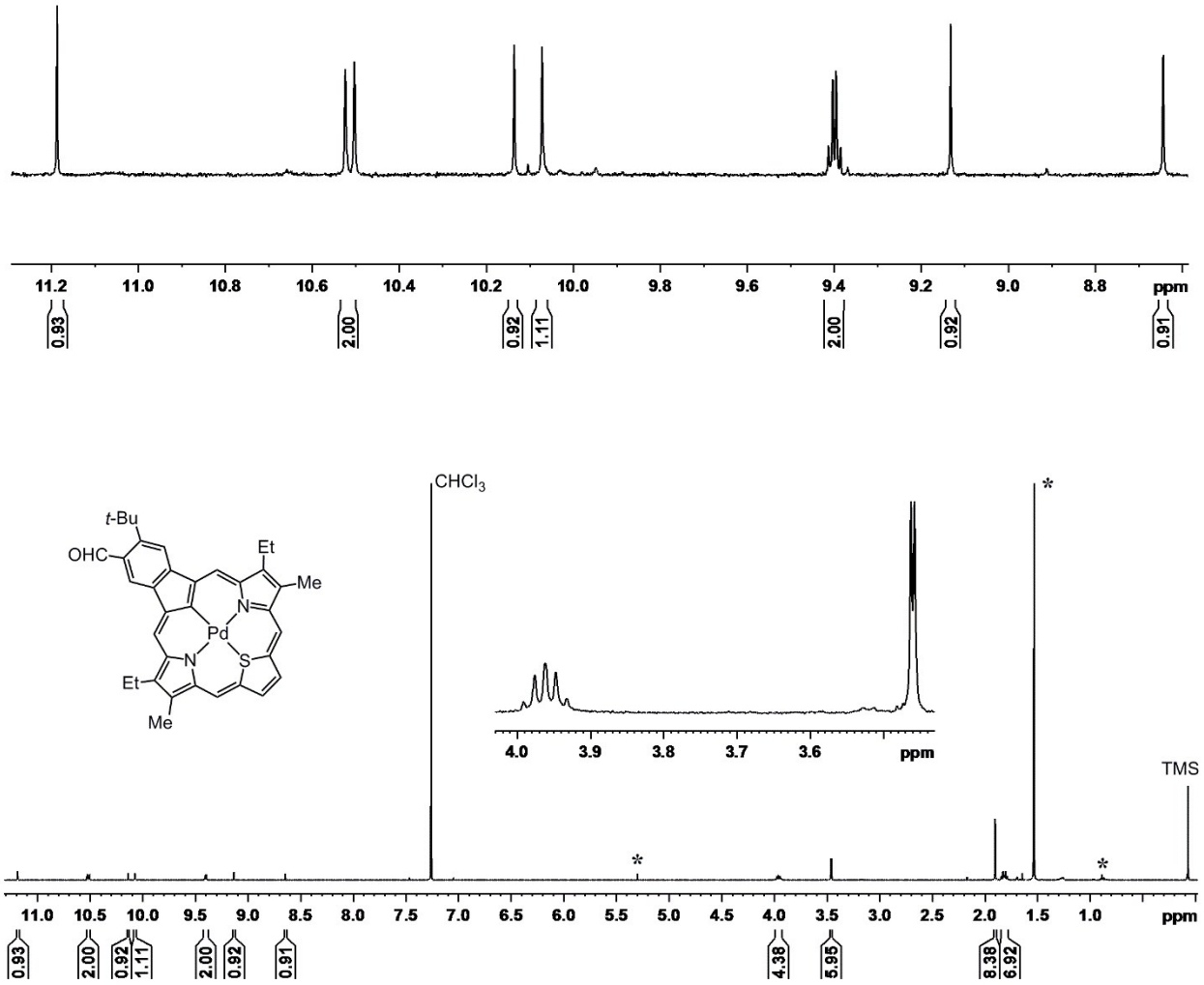

Figure S76. 500 MHz proton NMR spectrum of palladium(II) *tert*-butylbenzocarbaporphyrin carbaldehyde **29b** in $CDCl_3$.
* solvent impurities

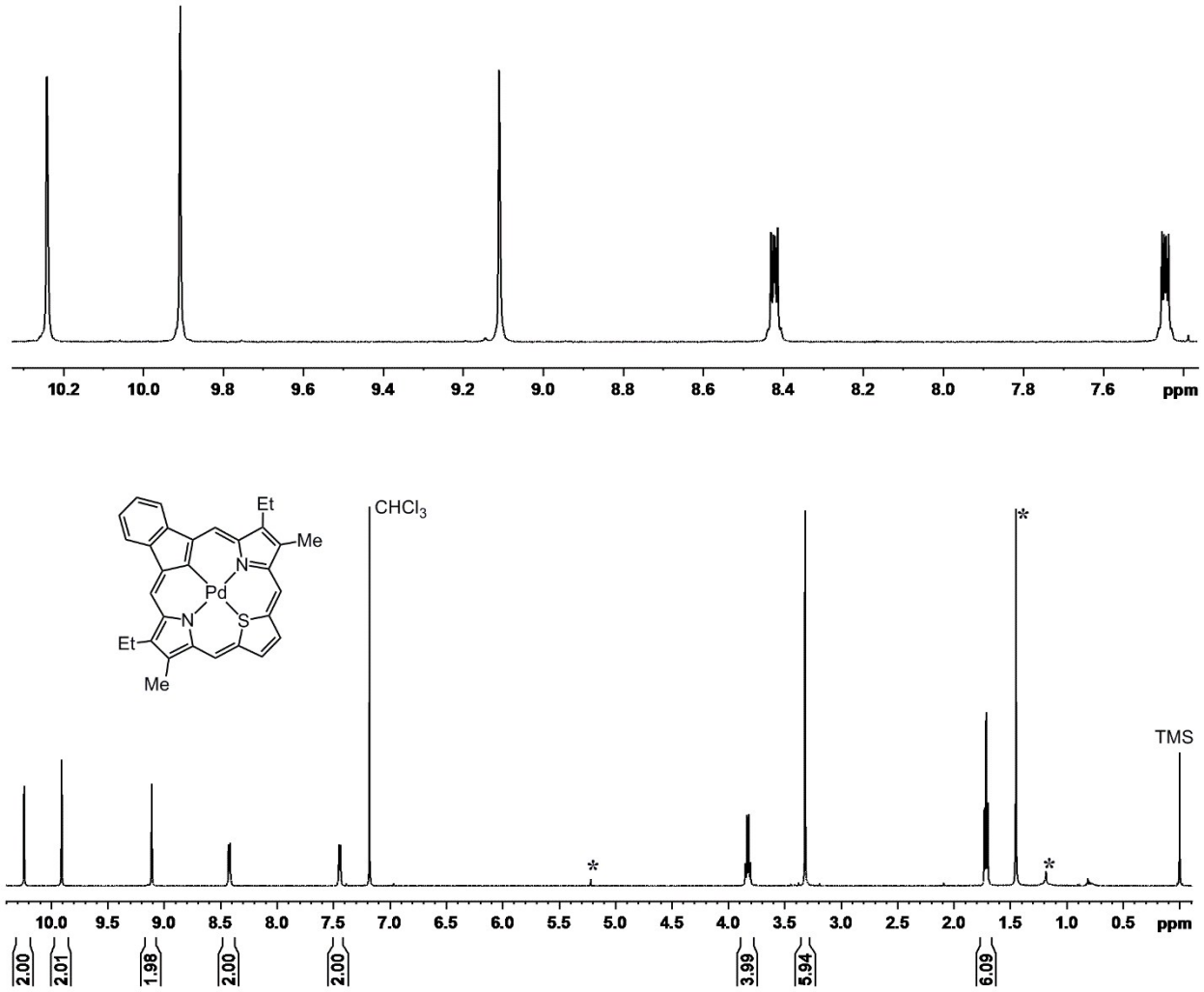

Figure S77. 500 MHz proton NMR spectrum of palladium(II) benzothiocarbaporphyrin **29c** in $CDCl_3$.

* solvent impurities

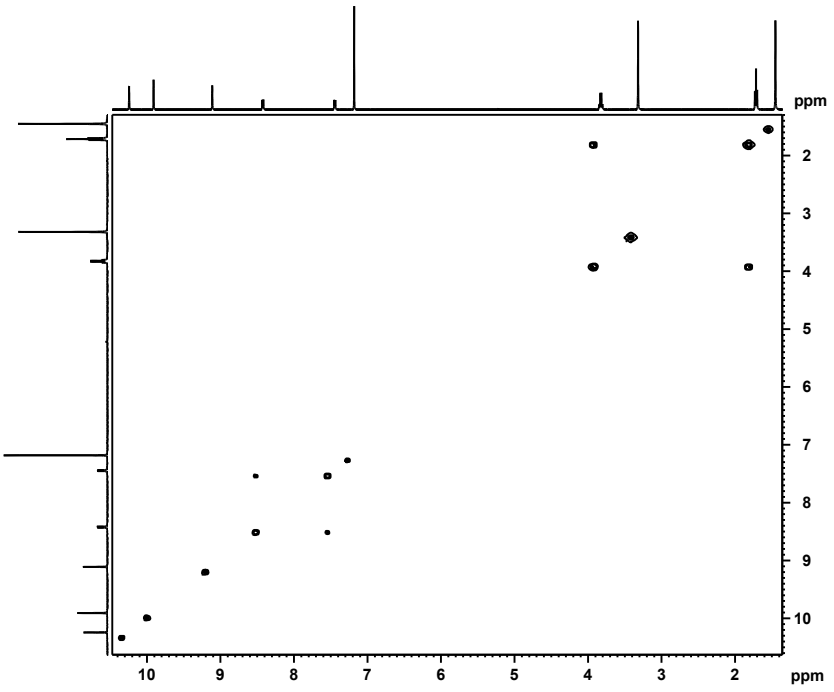

Figure S78. ^{1}H-^{1}H COSY NMR spectrum of **29c** in $CDCl_3$.

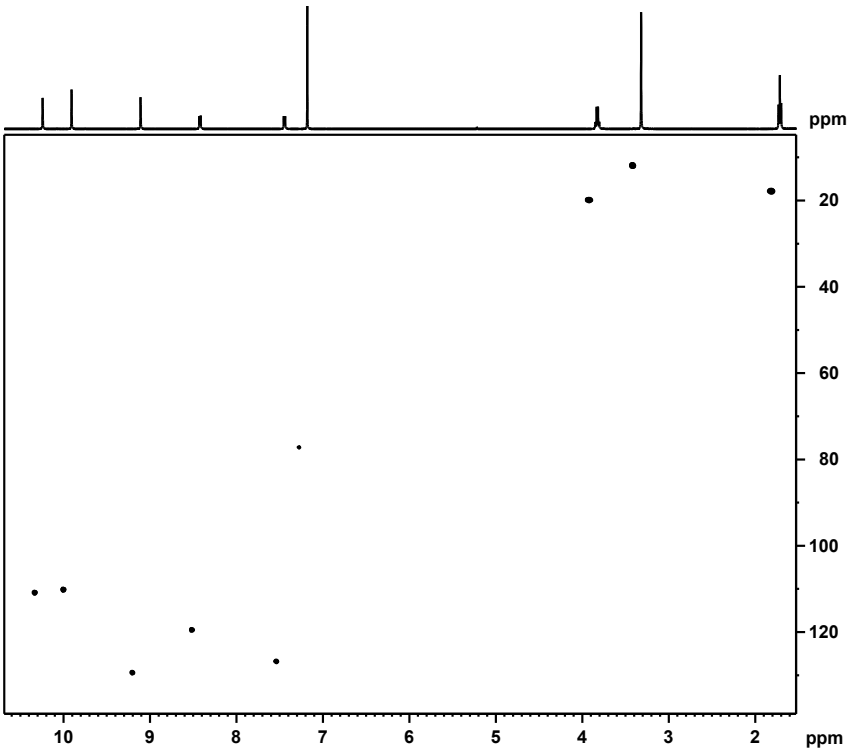

Figure S79. HSQC NMR spectrum of **29c** in $CDCl_3$.

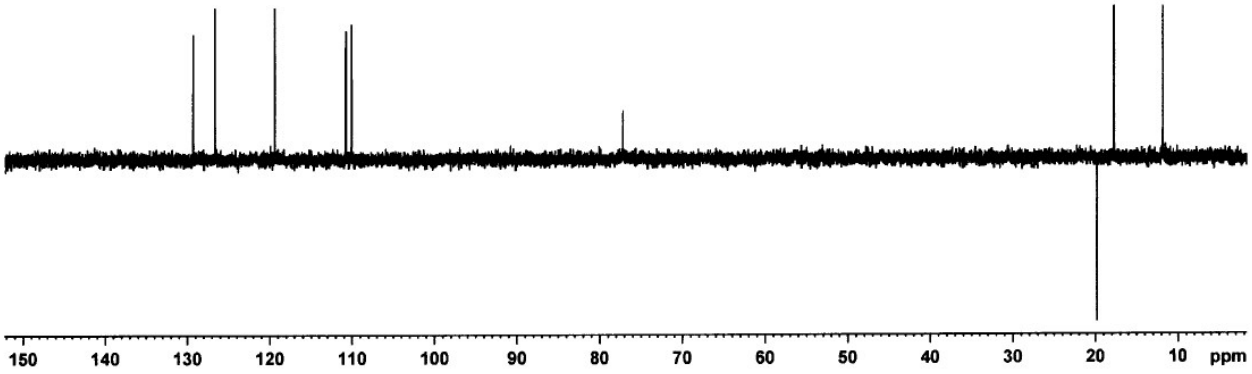

Figure S80. DEPT-135 NMR spectrum of **29c** in $CDCl_3$.

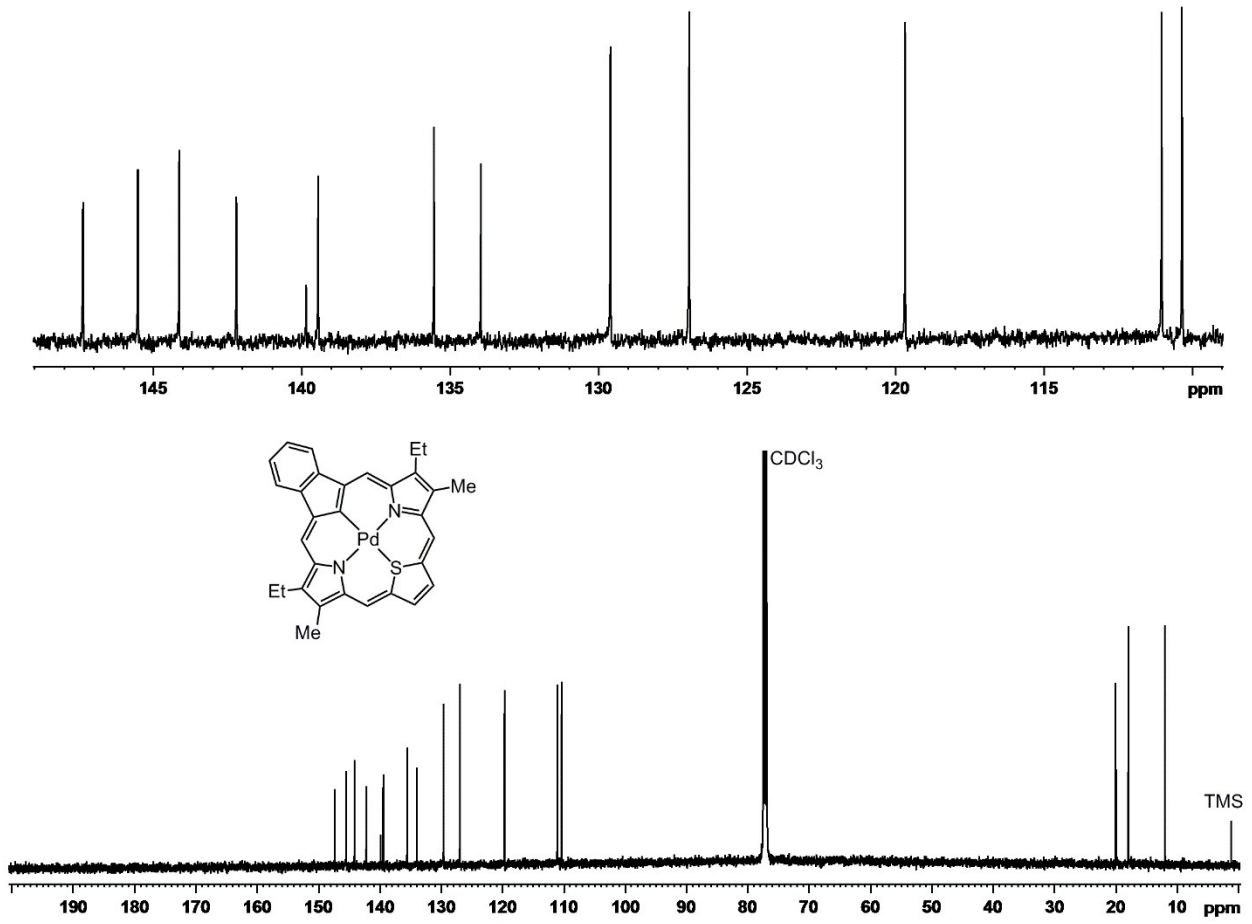

Figure S81. 125 MHz carbon-13 NMR spectrum of palladium(II) benzothiacarbaporphyrin **29c** in $CDCl_3$.

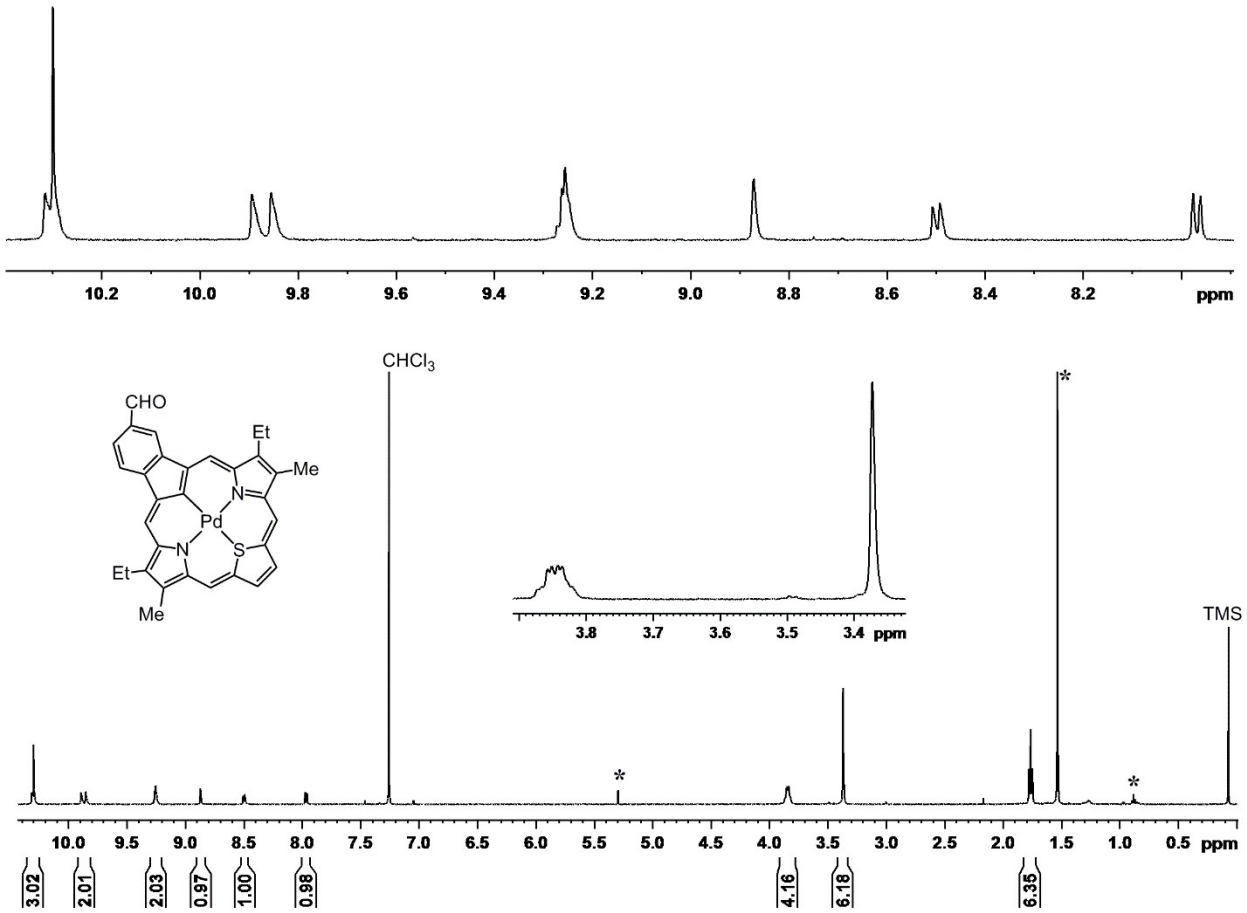

Figure S82. 500 MHz proton NMR spectrum of palladium(II) benzothiacarbaporphyrin **29d** in $CDCl_3$.

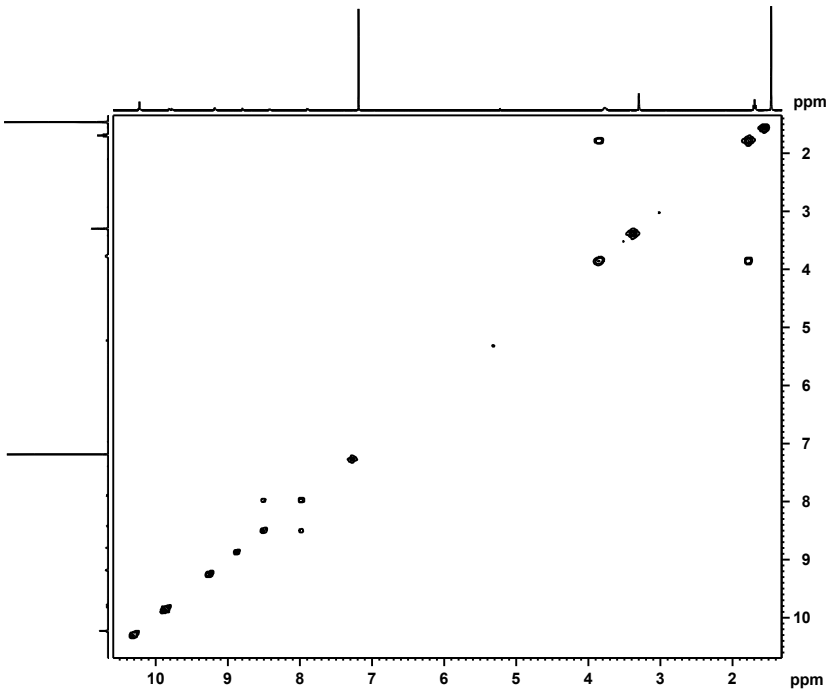

Figure S83. ^{1}H-^{1}H COSY NMR spectrum of palladium(II) benzothiacarbaporphyrin **29d** in $CDCl_3$.

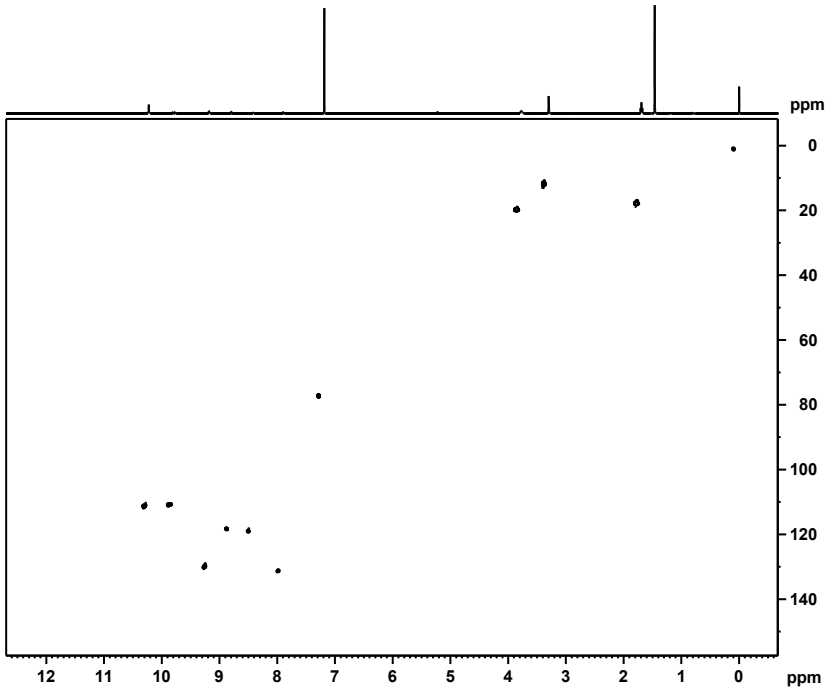

Figure S84. HSQC NMR spectrum of palladium(II) benzothiacarbaporphyrin **29d** in $CDCl_3$.

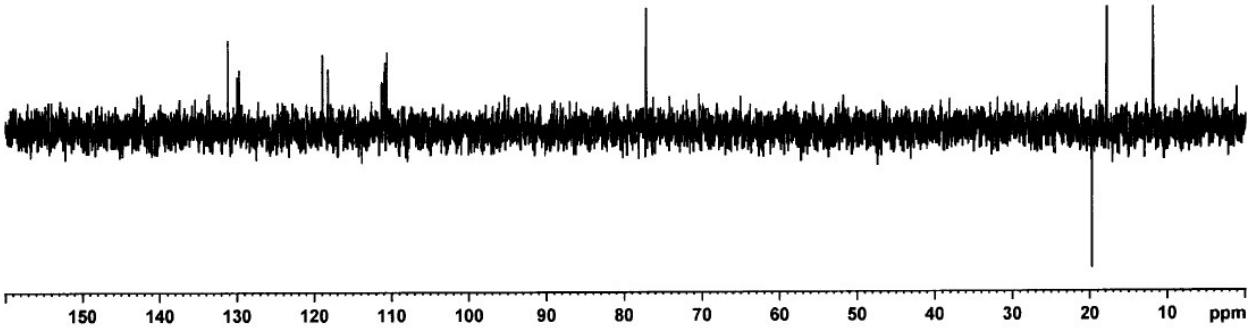

Figure S85. DEPT-135 NMR spectrum of palladium(II) benzothiacarbaporphyrin **29d** in $CDCl_3$.

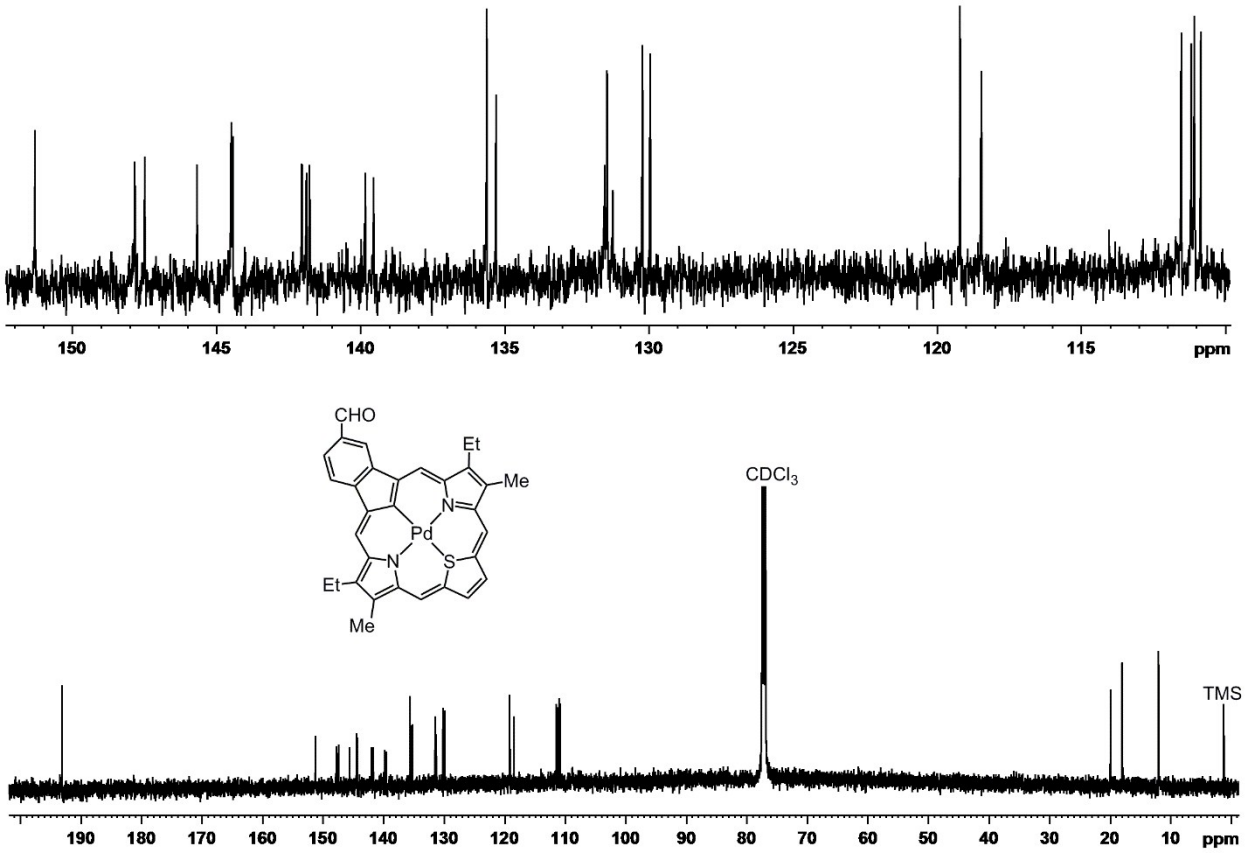

Figure S86. 125 MHz carbon-13 NMR spectrum of palladium(II) benzothiacarbaporphyrin **29d** in $CDCl_3$.

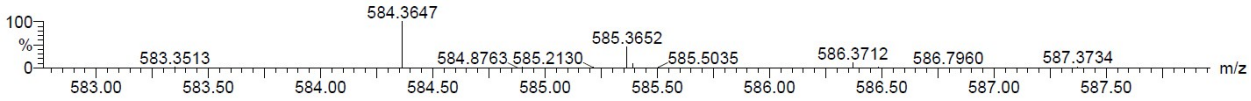

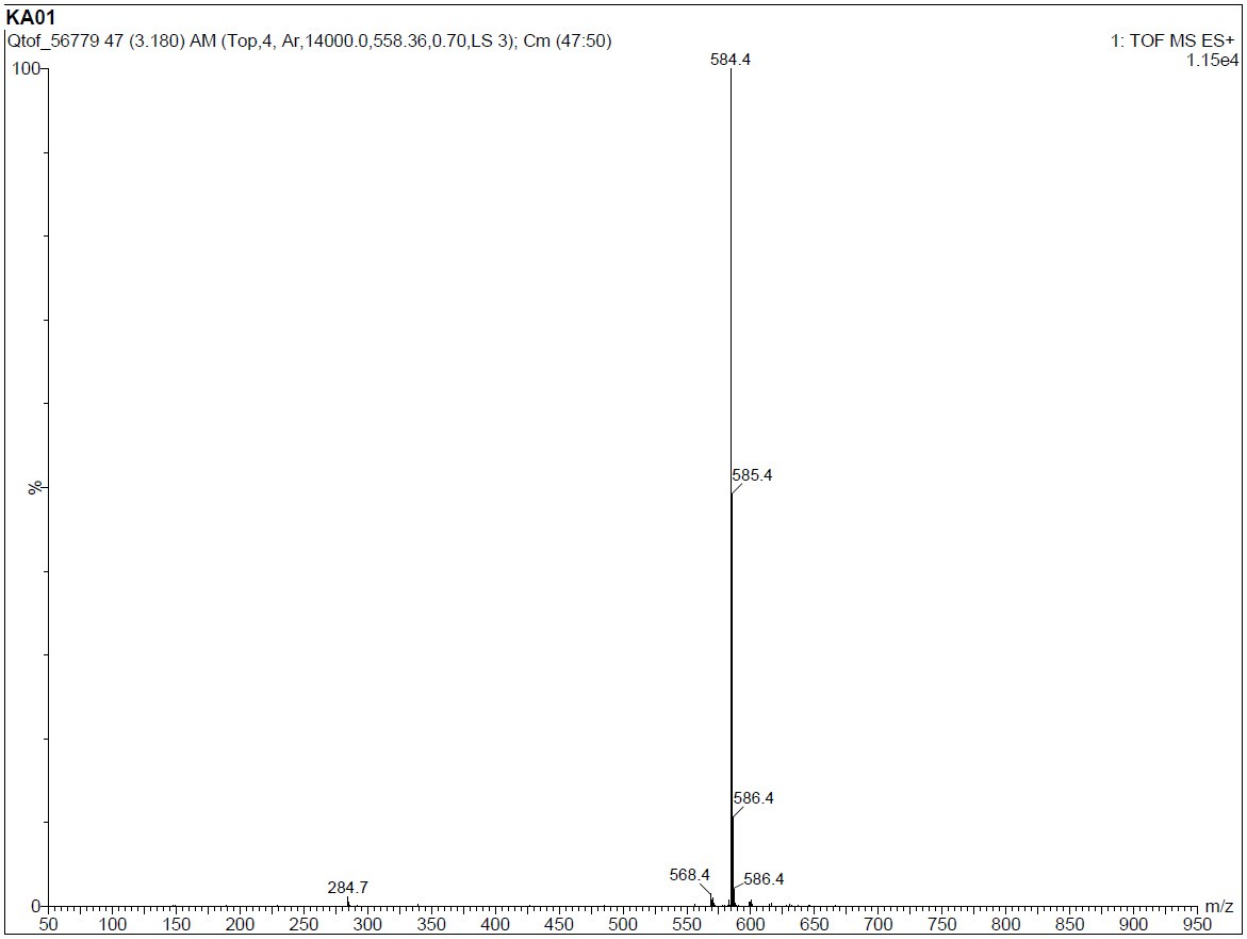

Figure S87. ESI MS of *tert*-butyl 21-oxyazuliporphyrin **16a**.

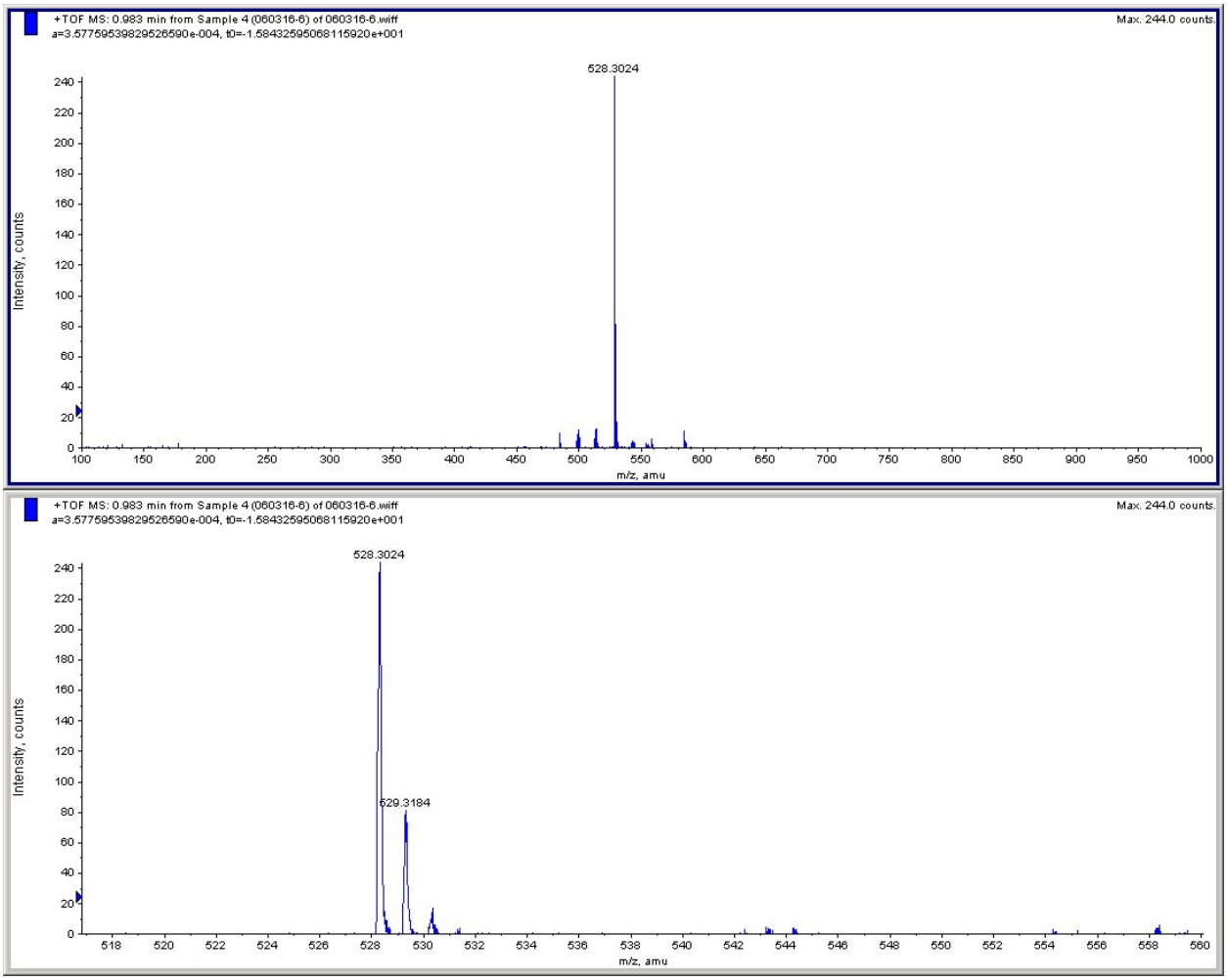

Figure S88. ESI MS of oxyazuliporphyrin **16b**.

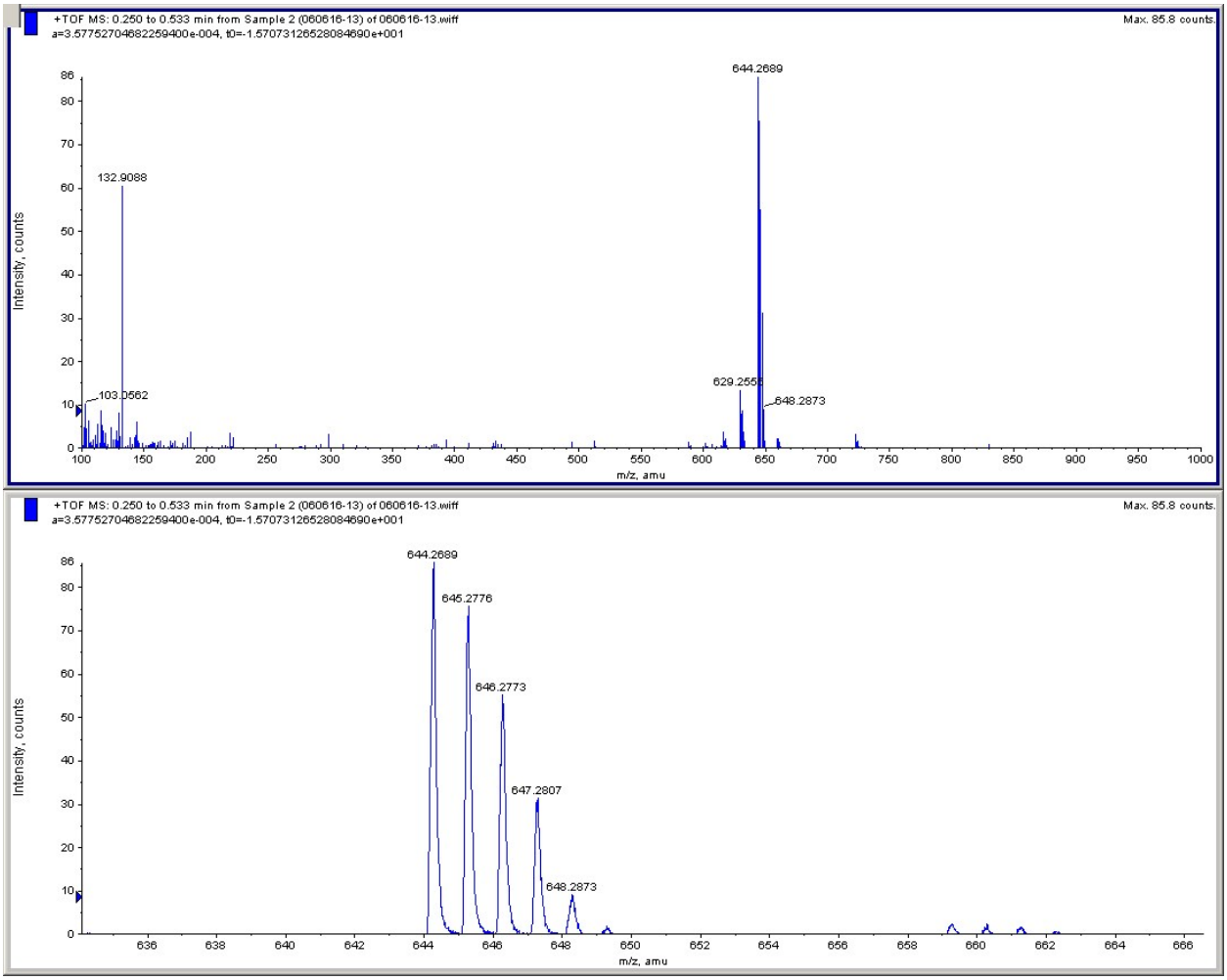

Figure S89. ESI MS of copper(II) complex **17a**.

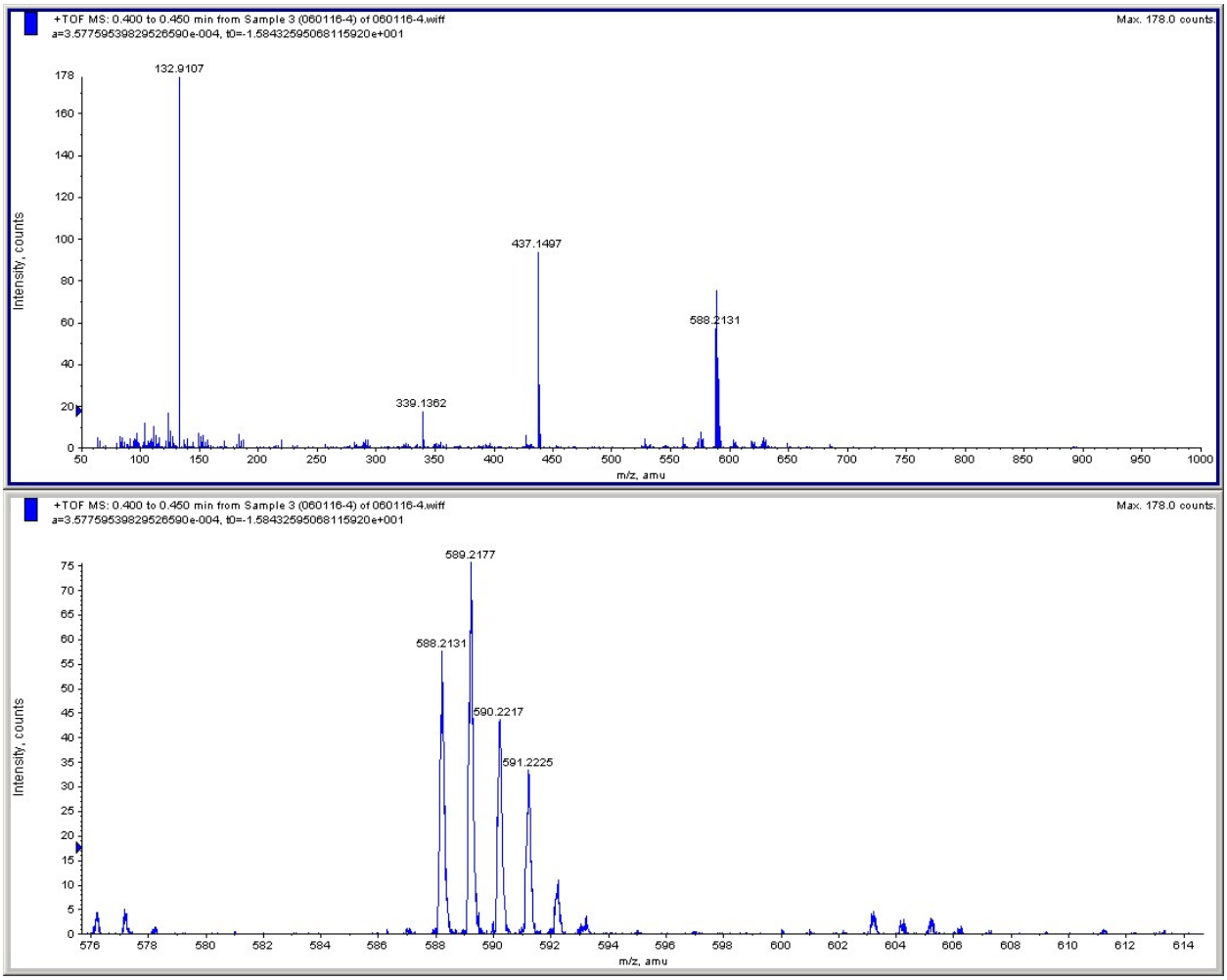

Scheme S90. ESI MS of copper(II) complex **17b**.

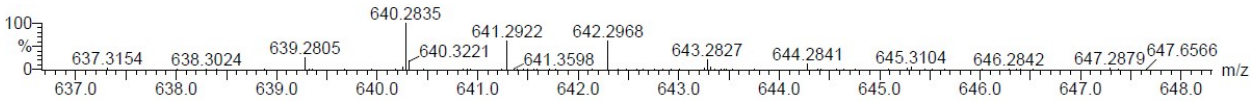

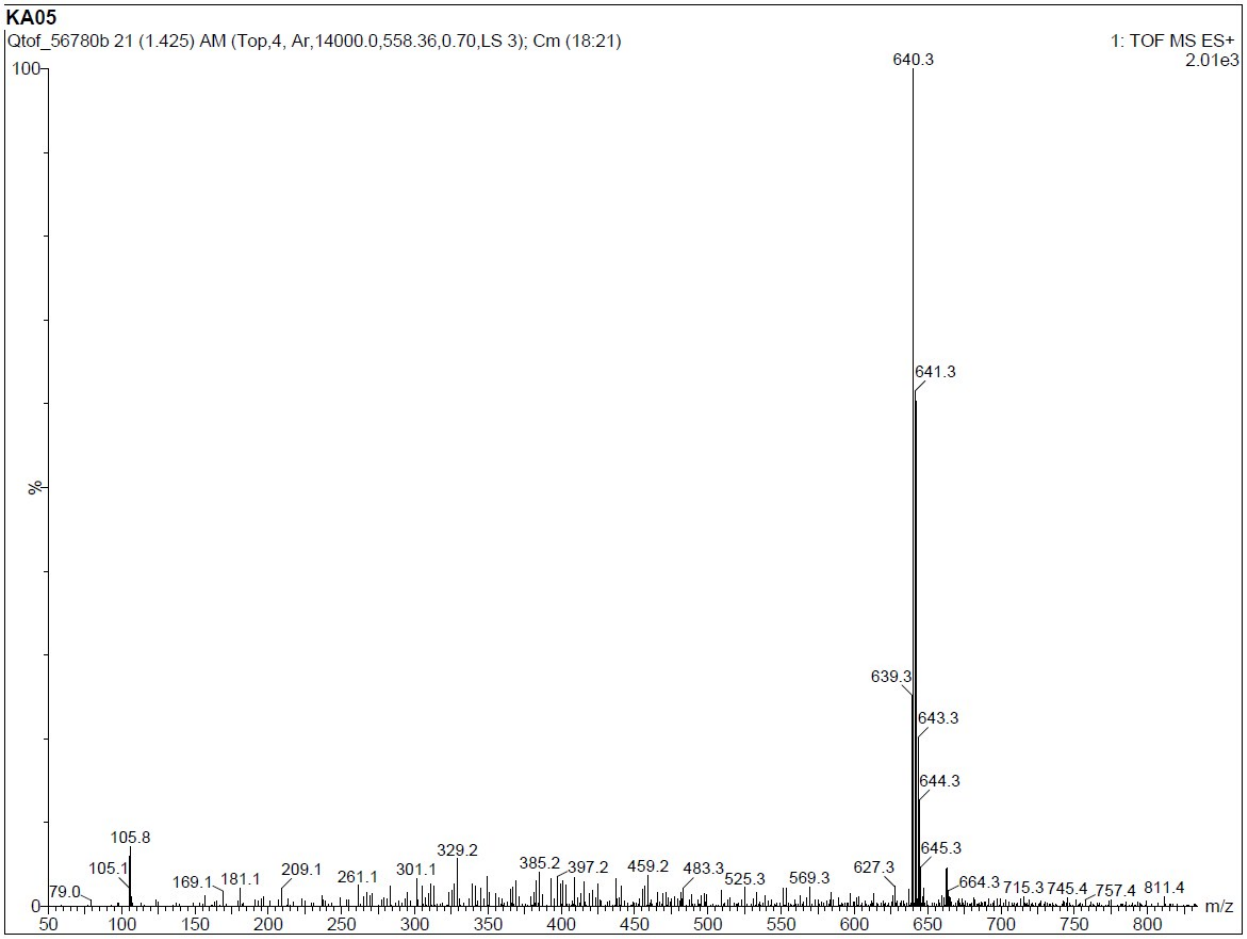

Scheme S91.ESI MS of nickel(II) complex **18a**.

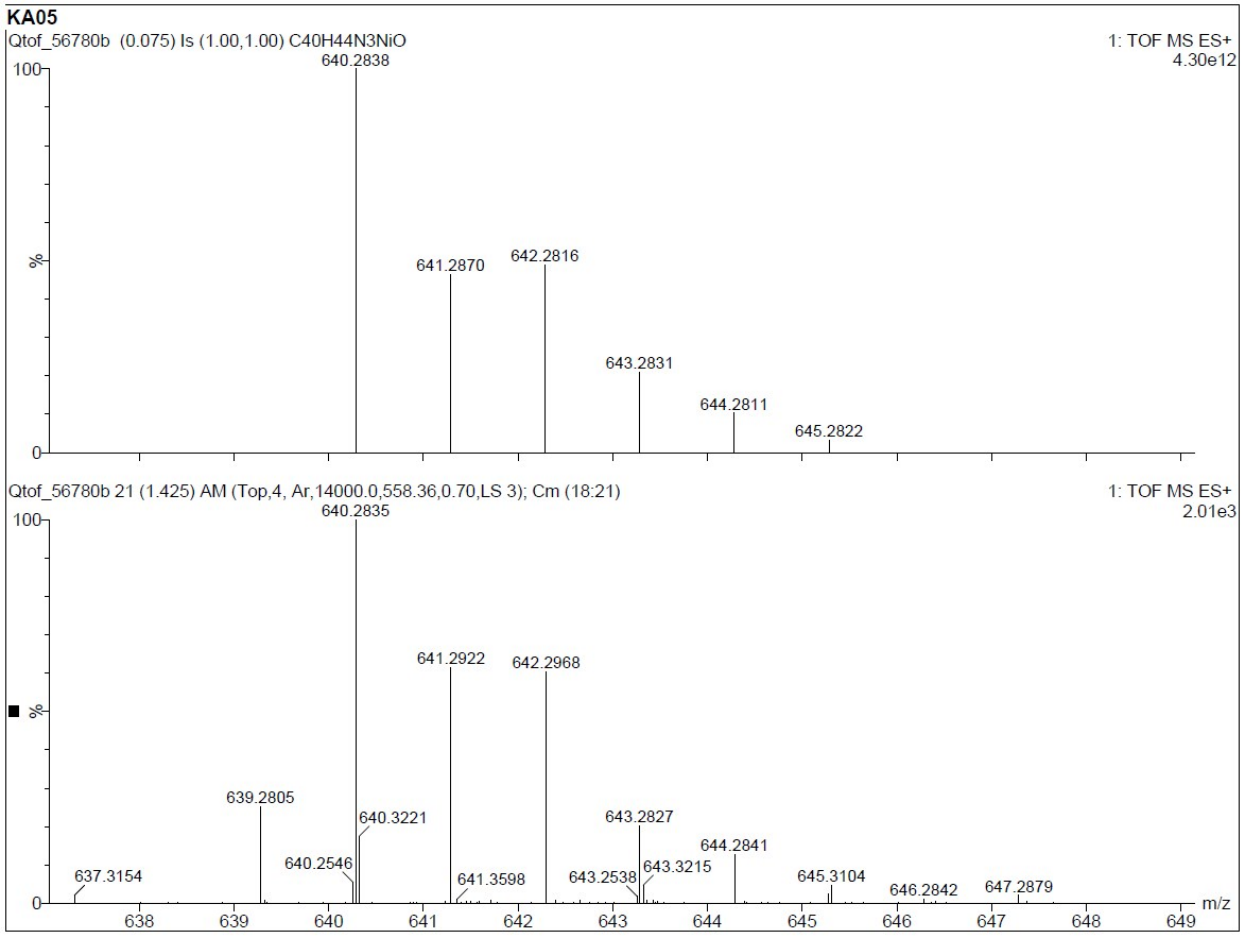

Figure S92. Analysis of the isotope peaks for the previous nickel complex.

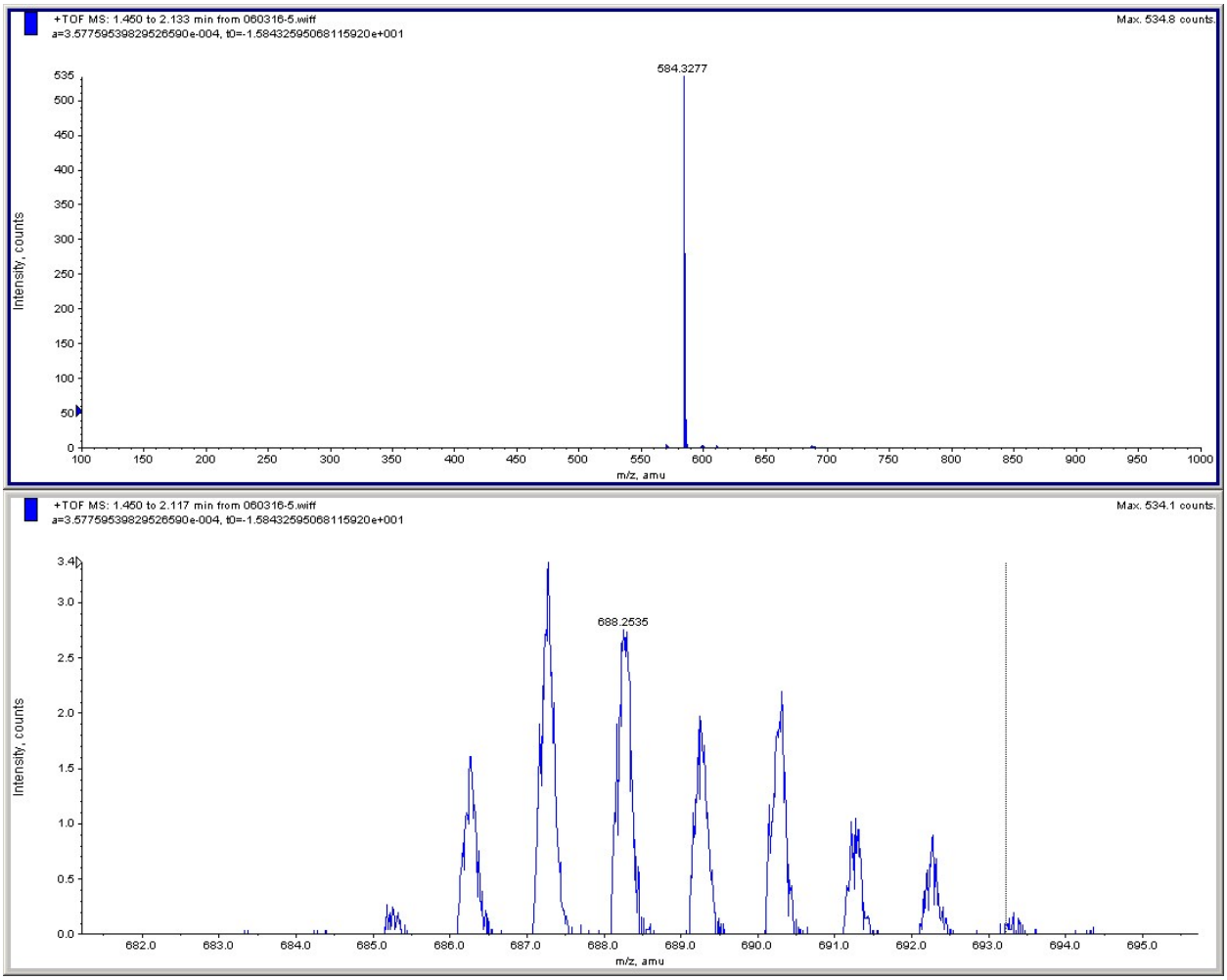

Figure S93. ESI MS of palladium(II) complex **18b**.

Selected Isotopes : C H $N_{0-3}Ag_{0-1}$ Error Limit : 5 ppm Unsaturation Limits : -.5 to 30

Measured Mass	*% Base*	*Formula*	*Calculated Mass*	*Error*	*Unsaturation*
659.2428	100.0%	$C_{39}H_{42}N_3Ag$	659.2430	-0.3	20.0

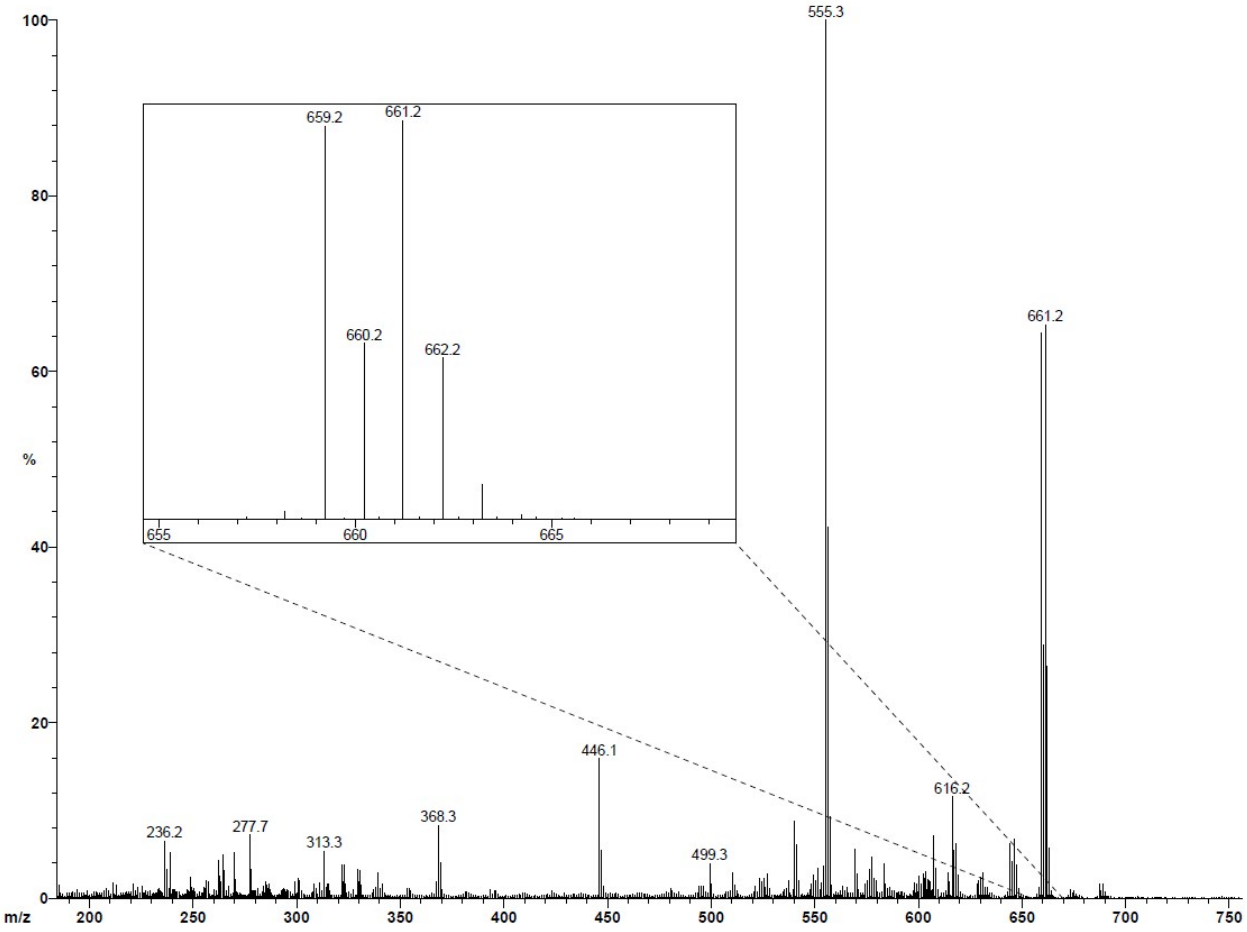

Figure S94. ESI MS of silver(III) *tert*-butylbenzocarbaporphyrin **21a**.

Selected Isotopes : C H N_{0-3} Ag_{0-1} O_{0-1} Error Limit : 5 ppm Unsaturation Limits : -.5 to 30

Measured Mass	*% Base*	*Formula*	*Calculated Mass*	*Error*	*Unsaturation*
687.2376	100.0%	$C_{40}H_{42}N_3AgO$	687.2379	-0.4	21.0

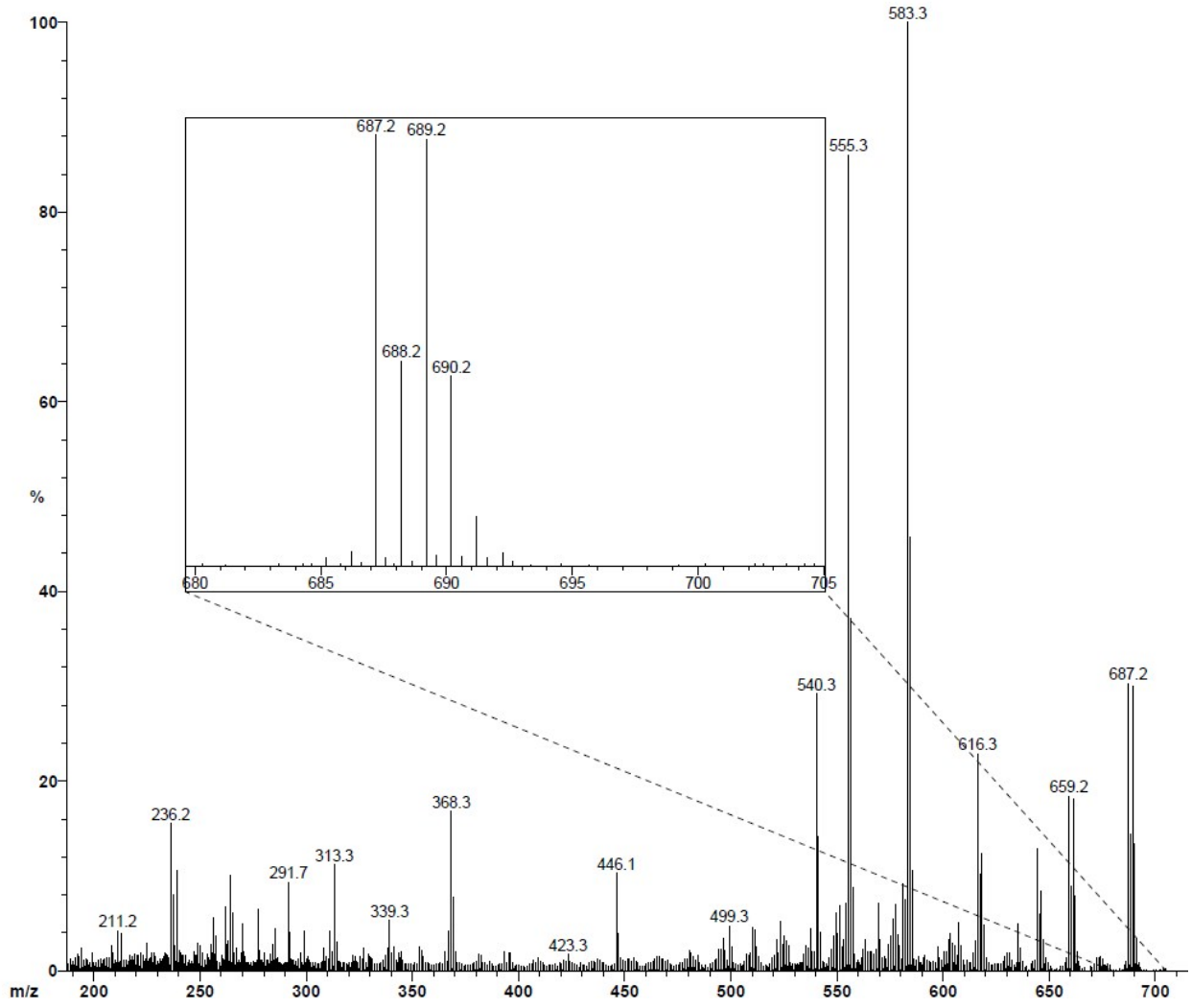

Figure S95. ESI MS of silver(III) *tert*-butylbenzocarbaporphyrin carbaldehyde **21b**.

Selected Isotopes : C H $N_{0-3}Ag_{0-1}O_{0-1}$ Error Limit : 5 ppm Unsaturation Limits : -.5 to 30

Measured Mass	*% Base*	*Formula*	*Calculated Mass*	*Error*	*Unsaturation*
631.1731	31.2%	$C_{36}H_{34}N_3AgO$	631.1753	-3.5	21.0

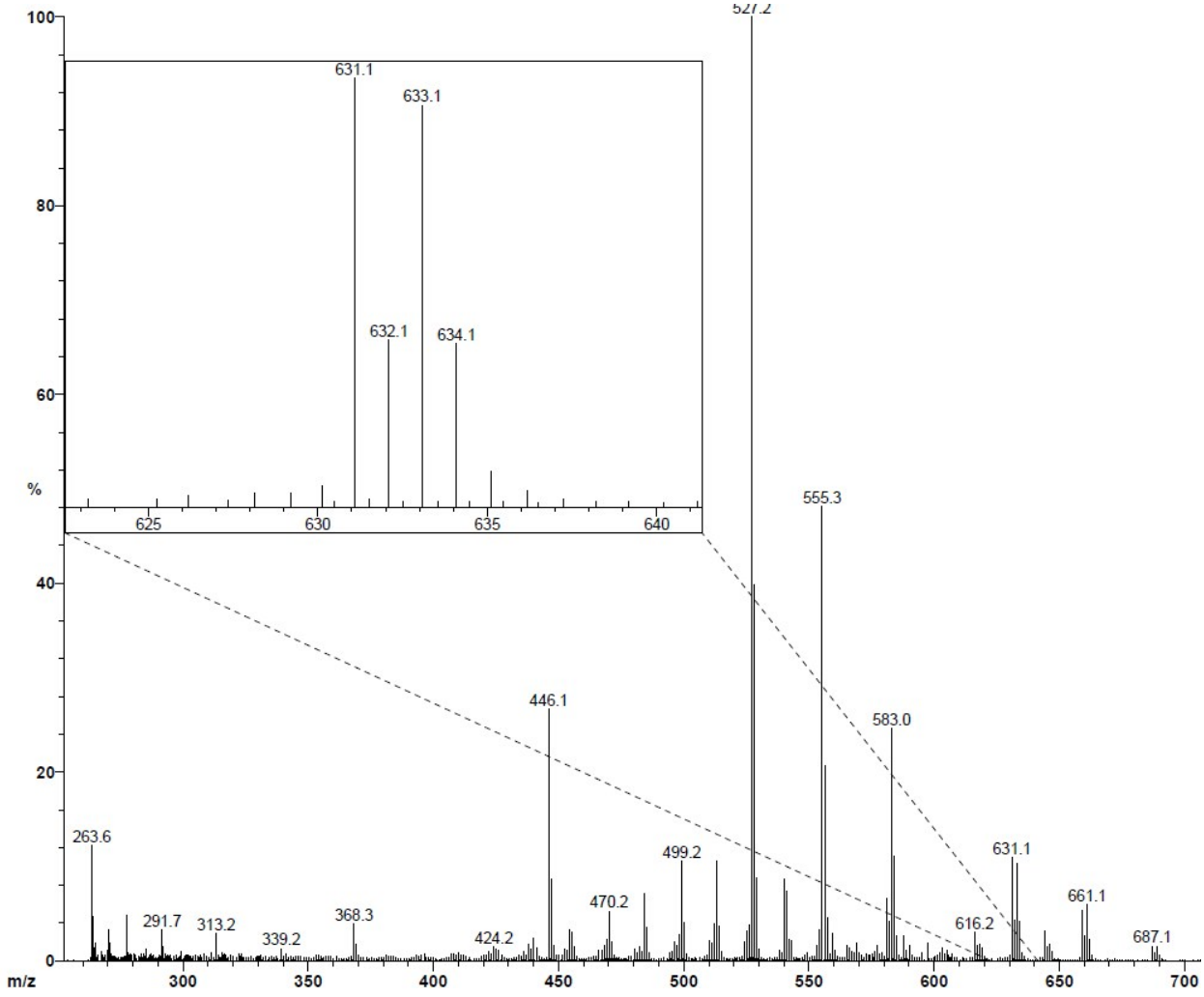

Figure S96. ESI MS of silver(III) benzocarbaporphyrin 2[1]-carbaldehyde **22c**.

Selected Isotopes : C H $O_{0-1}N_{0-4}Ag_{0-1}$ Error Limit : 5 ppm Unsaturation Limits : -.5 to 30

Measured Mass	*% Base*	*Formula*	*Calculated Mass*	*Error*	*Unsaturation*
631.1763	4.0%	$C_{36}H_{34}O N_3Ag$	631.1753	1.6	21.0

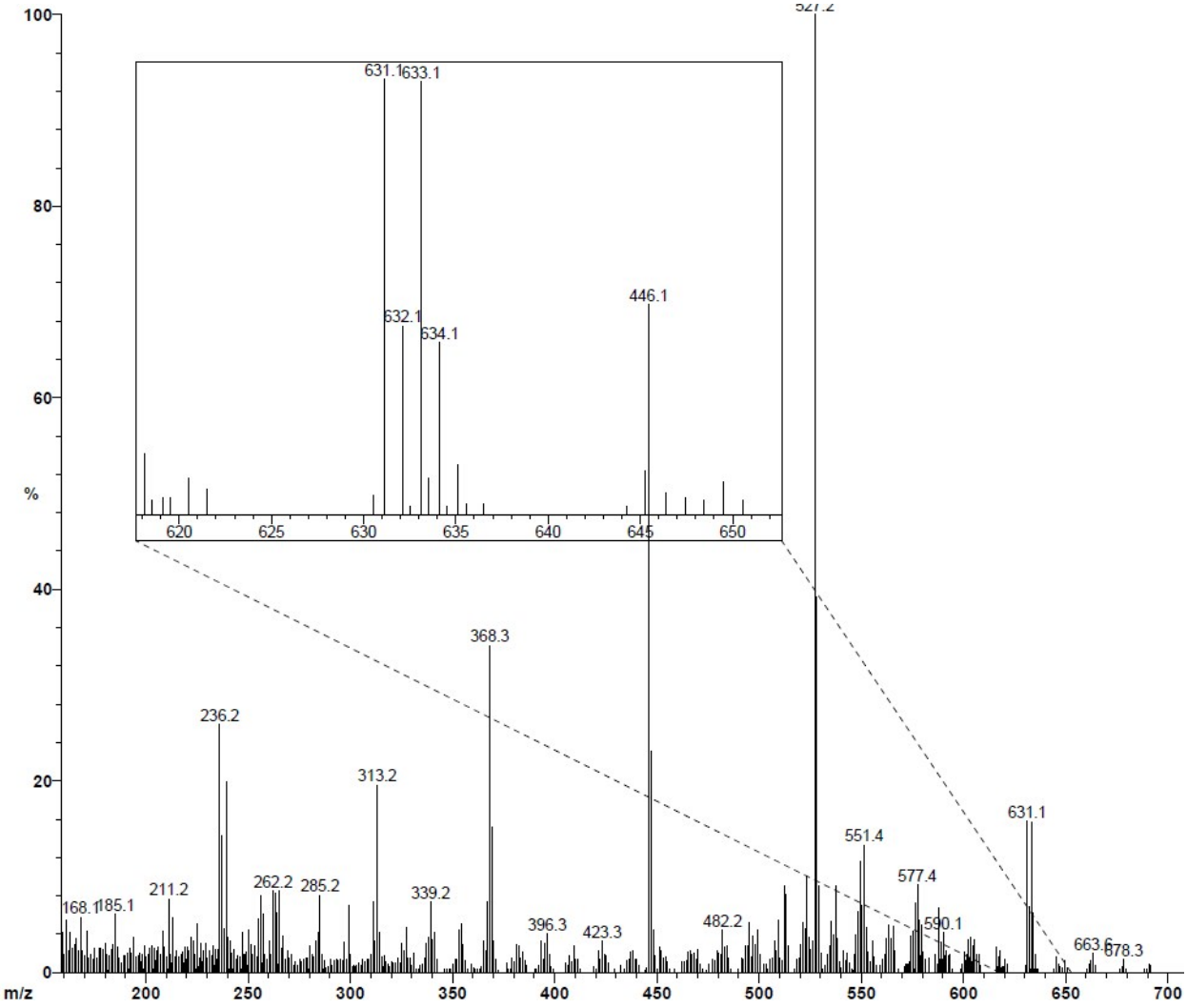

Figure S97. ESI MS of silver(III) benzocarbaporphyrin 2^2-carbaldehyde **22b**.

Selected Isotopes : C H $O_{0-1}N_{0-4}Ag_{0-1}$ Error Limit : 5 ppm Unsaturation Limits : -.5 to 30

Measured Mass	*% Base*	*Formula*	*Calculated Mass*	*Error*	*Unsaturation*
603.1816	17.8%	$C_{37}H_{36}O$ Ag	603.1817	-0.2	19.5
		$C_{35}H_{34}N_3$Ag	603.1804	2.0	20.0

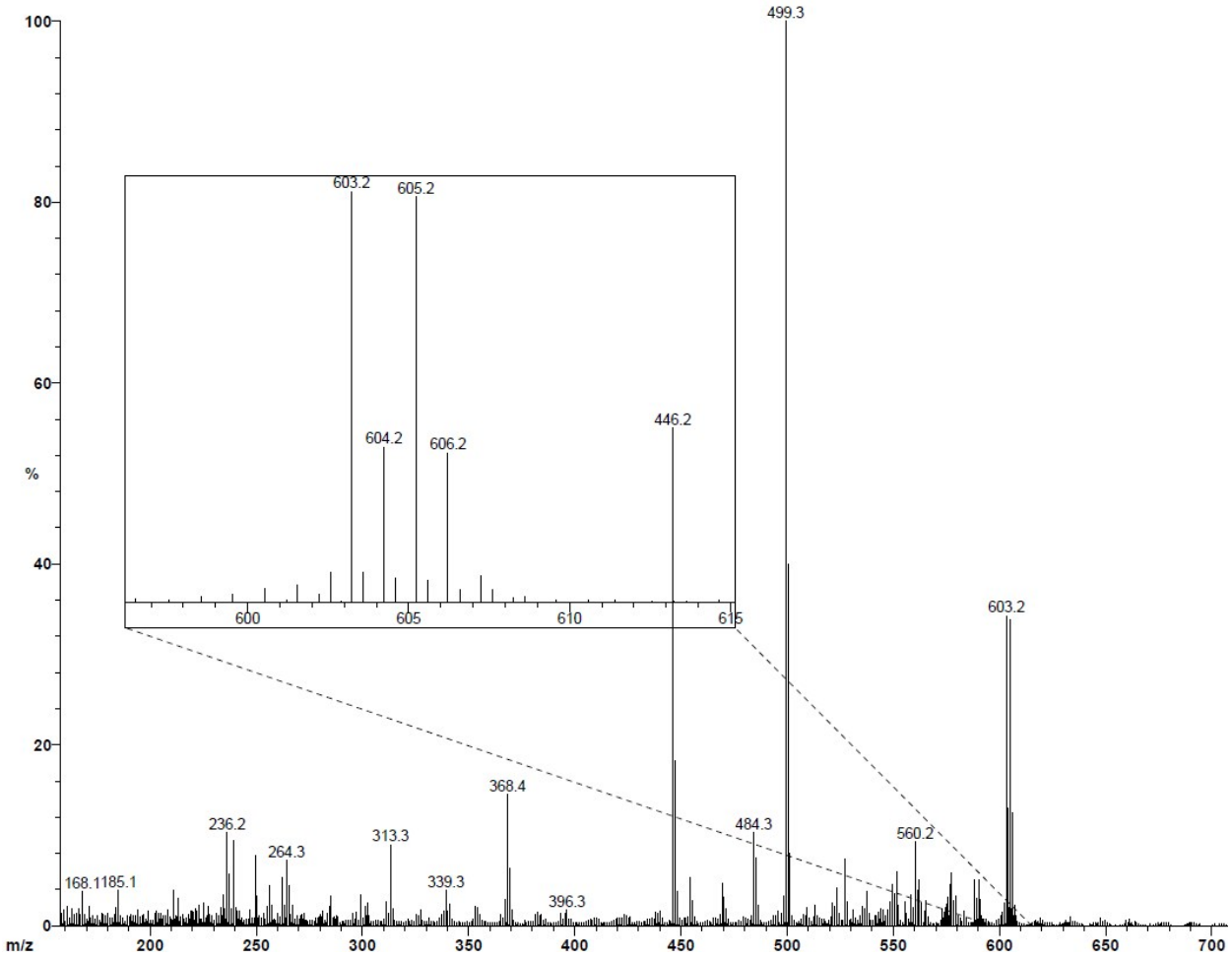

Figure S98. ESI MS of silver(III) benzocarbaporphyrin **22a.**

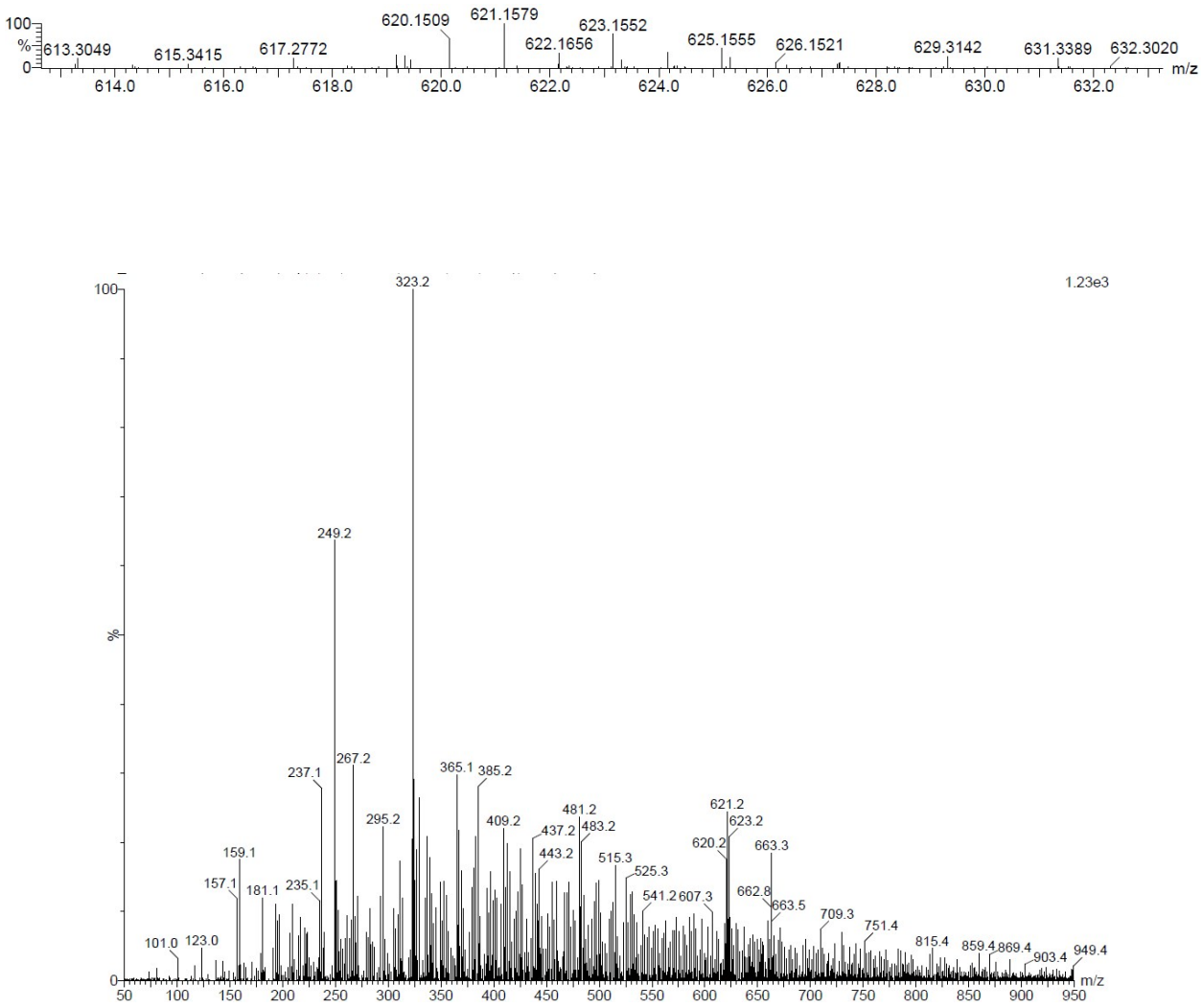

Figure S99. ESI MS of palladium(II) *tert*-butylbenzothiocarbaporphyrin **29a.**

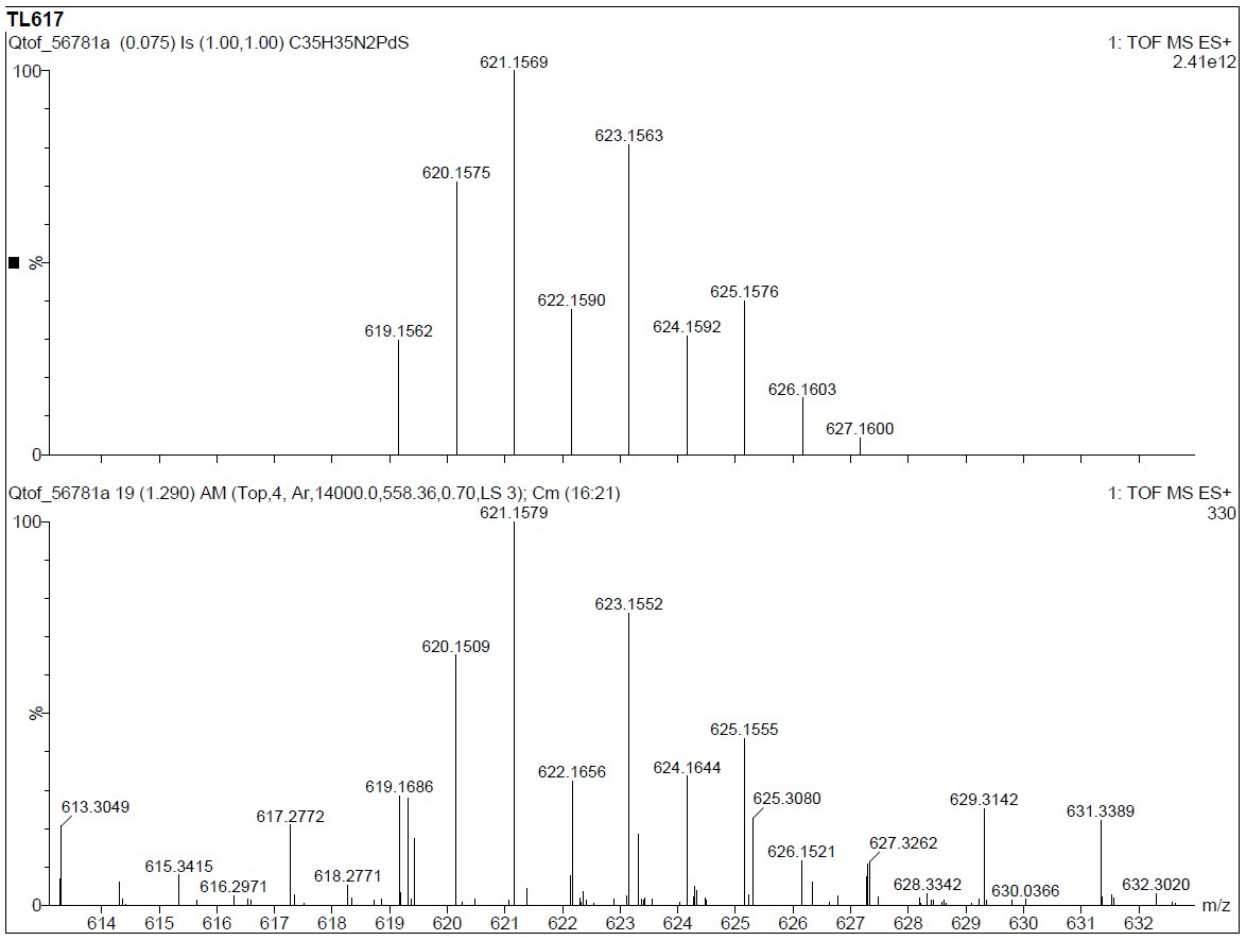

Figure S100. Analysis of the isotope peaks for the previous palladium complex.

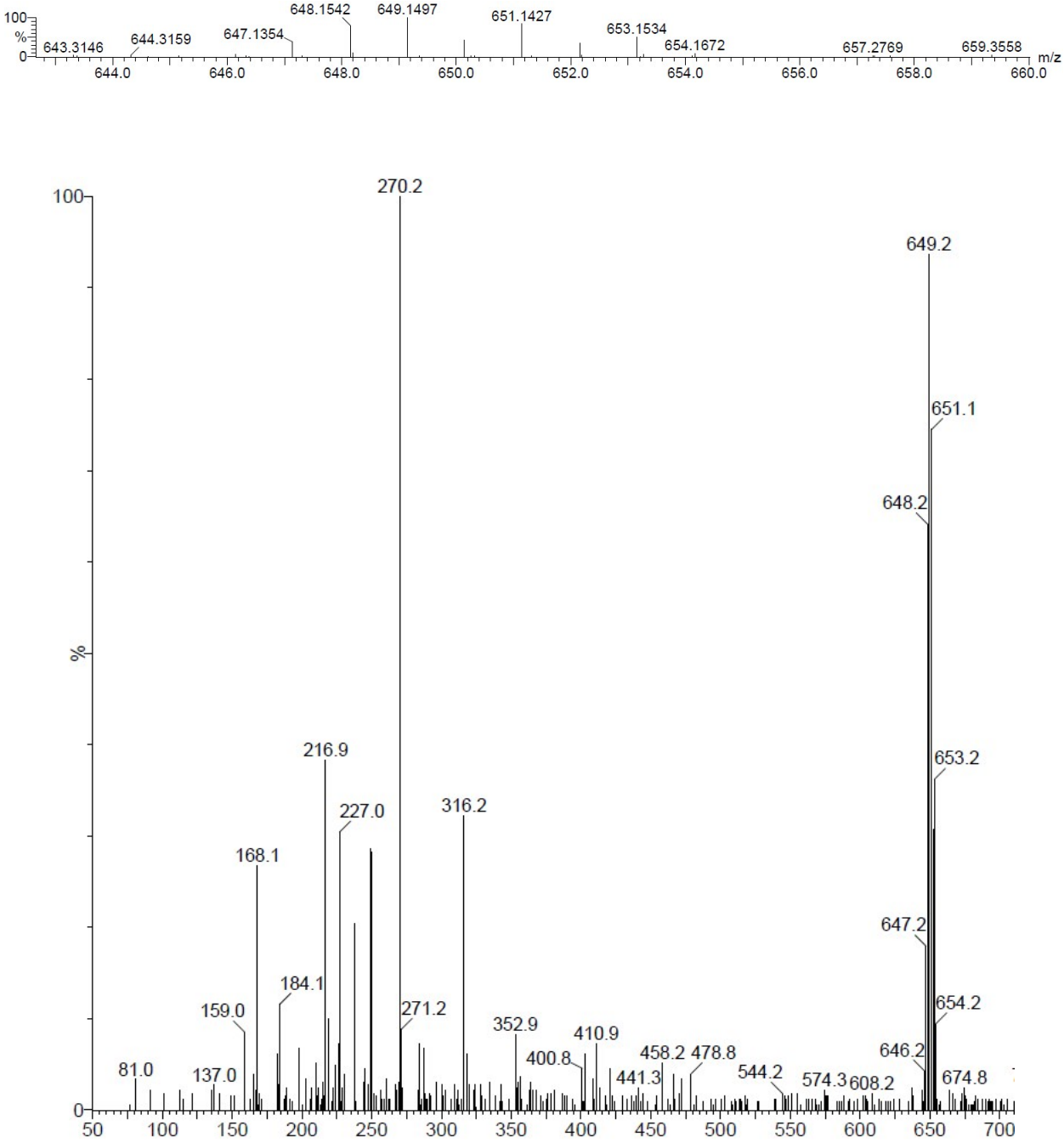

Figure S101. ESI MS of palladium(II) *tert*-butylbenzothiocarbaporphyrin carbaldehyde **29b.**

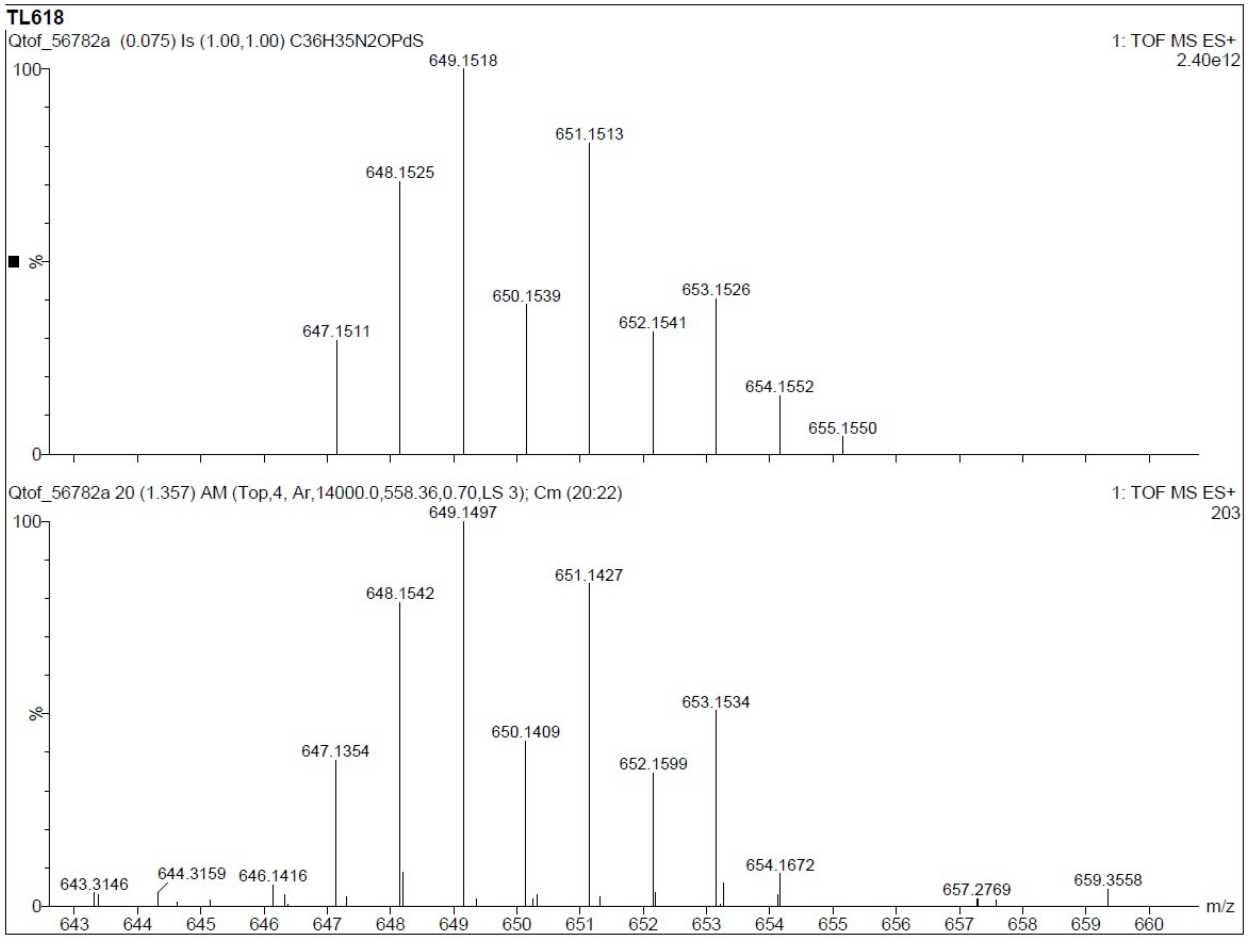

Figure S102. Analysis of the isotope peaks for the previous palladium complex.

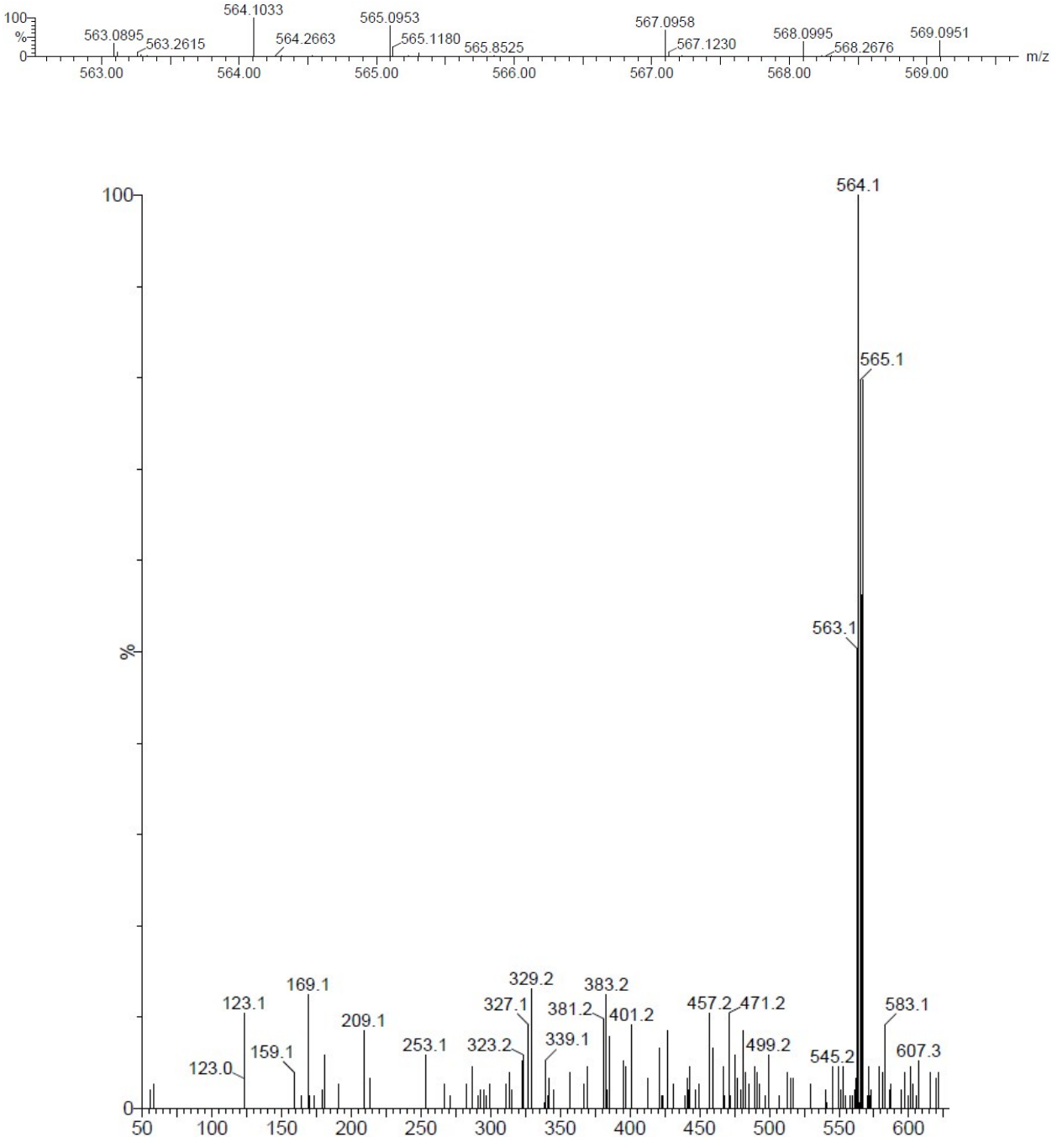

Figure S103. ESI MS of palladium(II) benzothiocarbaporphyrin **29c.**

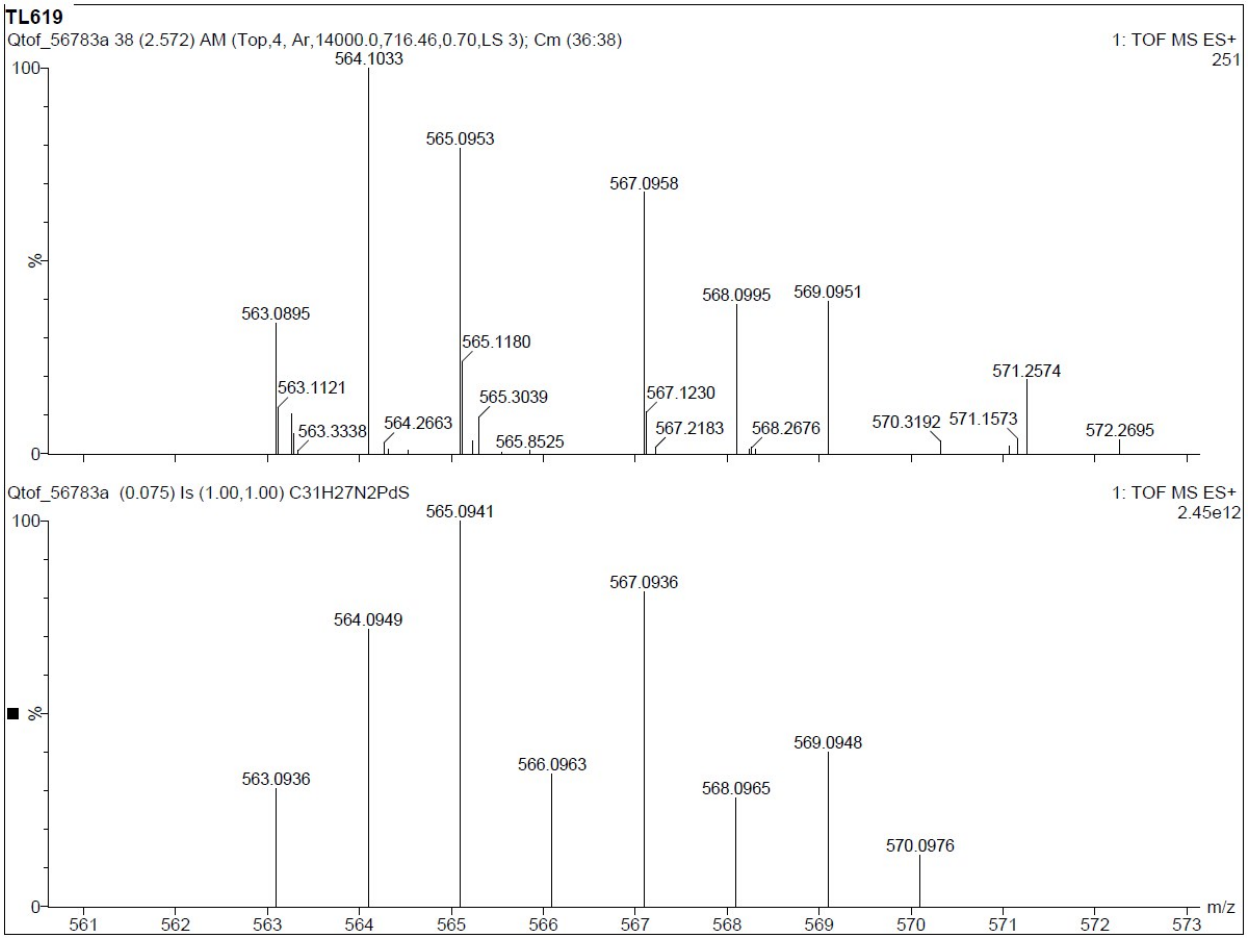

Figure S104. Analysis of the isotope peaks for the previous palladium complex.

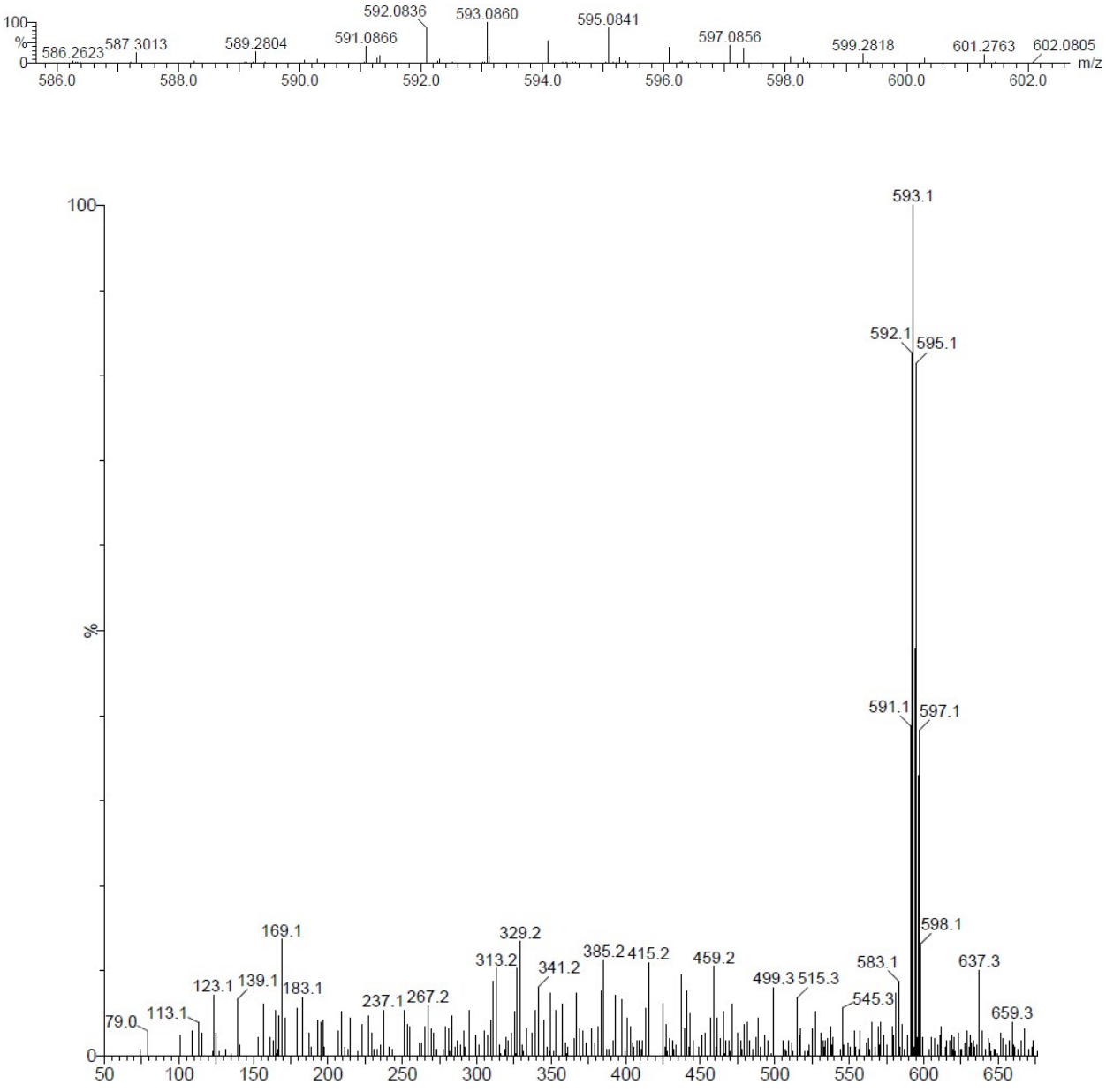

Figure S105. ESI MS of palladium(II) benzothiocarbaporphyrin carbaldehyde **29d.**

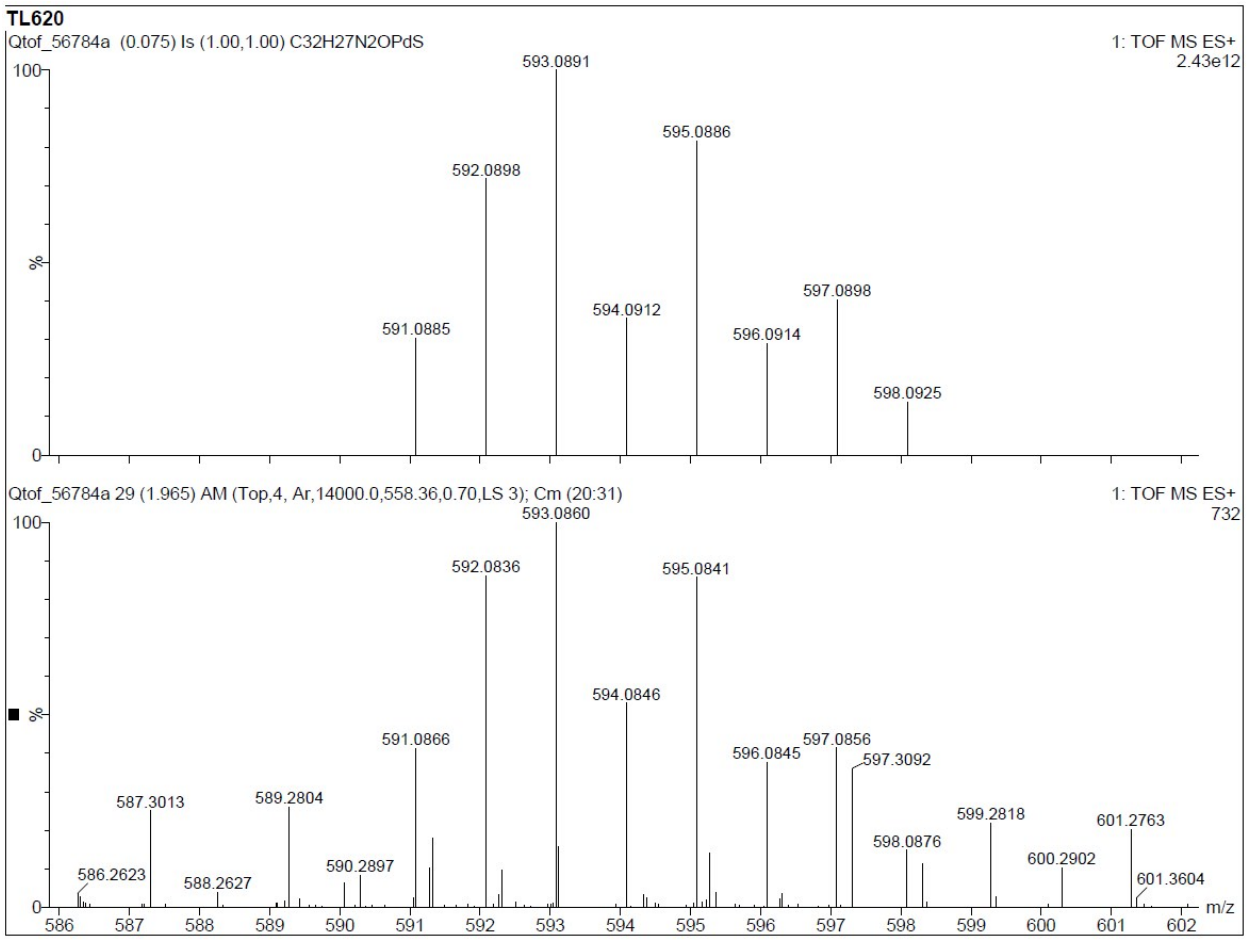

Figure S106. Analysis of the isotope peaks for the previous palladium complex.